MAL2 drives immune evasion in breast cancer by suppressing tumor antigen presentation

Yuanzhang Fang, Lifei Wang, Changlin Wan, Yifan Sun, Kevin Van der Jeught, Zhuolong Zhou, Tianhan Dong, Kaman So, Tao Yu, Yujing Li, Haniyeh Eyvani, Austin B Colter, Edward Dong, Sha Cao, Jin Wang, Bryan P Schneider, George E Sandusky, Yunlong Liu, Chi Zhang, Xiongbin Lu, Xinna Zhang

Inventory of Supplementary Information

Supplemental Figure 1

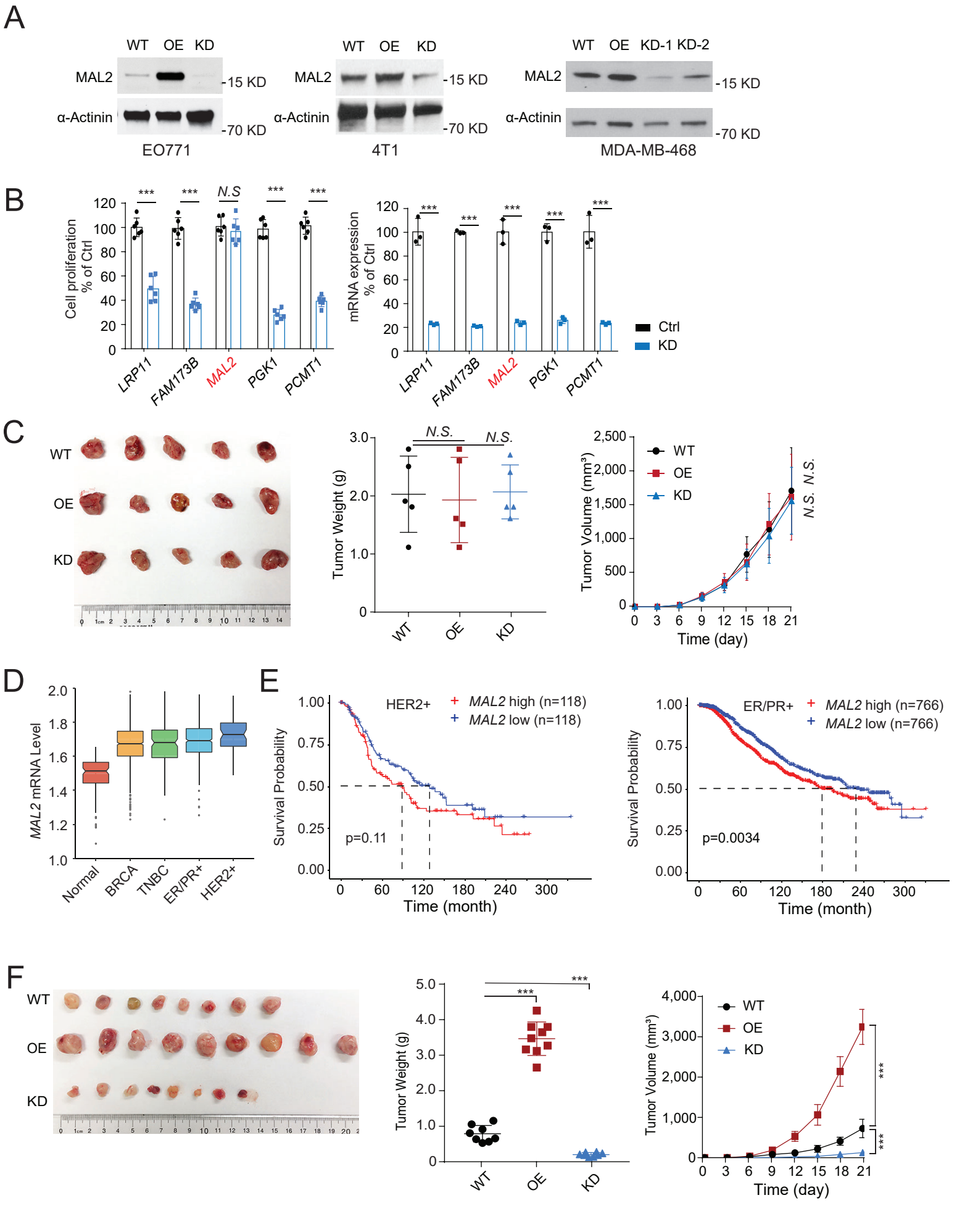

Supplemental Figure 1. MAL2 drives breast tumor growth in immunocompetent models. (**A**) MAL2 expression levels in tumor cells with *MAL2* overexpressed or silenced. α-Actinin was used as a loading control. (**B**) Knockdown of *LRP11*, *FAM173B*, *PGK1* or *PCMT1* inhibited the proliferation of breast cancer cells, but knockdown of *MAL2* had no effect on the cancer cell proliferation. MDA-MB-468 cells were used in the studies for *LRP11*, *FAM173B*, and *MAL2*, and HCC1954 cells were used in the studies for *PGK1* and *PCMT1*. (**C**) 4T1 cells with different *Mal2* expression levels (n = 5 per group) were orthotopically transplanted separately into 5-week-old female NU/J mice (5×10^4 cells per mouse). Mice were euthanized 21 days after the injection and the tumors were collected, weighted and measured. Data are presented as mean ± SD. One-way and two-way ANOVA tests were used for data analysis in tumor weight and tumor growth, respectively. (**D**) *MAL2* gene is highly expressed in all subtypes of human breast cancer. One-way ANOVA test was used for statistical analysis of TCGA breast cancer datasets. (**E**) High expression of *MAL2* is correlated with poor survival of breast cancer patients. Kaplan-Meier analysis was conducted for overall survival in patients with HER2+ and ER/PR+ breast cancers. Clinical data from TCGA and METABRIC cohorts were combined in the analyses. Log-rank test was used for statistical analysis. (**F**) 4T1 cells with different *Mal2* expression levels were orthotopically transplanted into 5-week-old female C57BL/6 mice (5×10^4 cells per mouse). Mice were euthanized 21 days after the injection and the tumors were collected, weighted and measured. Data are presented as mean ± SD. One-way and two-way ANOVA tests were used for data analysis in tumor weight and tumor growth, respectively. *, $p<0.05$; **, $p<0.01$; ***, $p<0.001$; *N.S.*, no significance.

Supplemental Figure 2

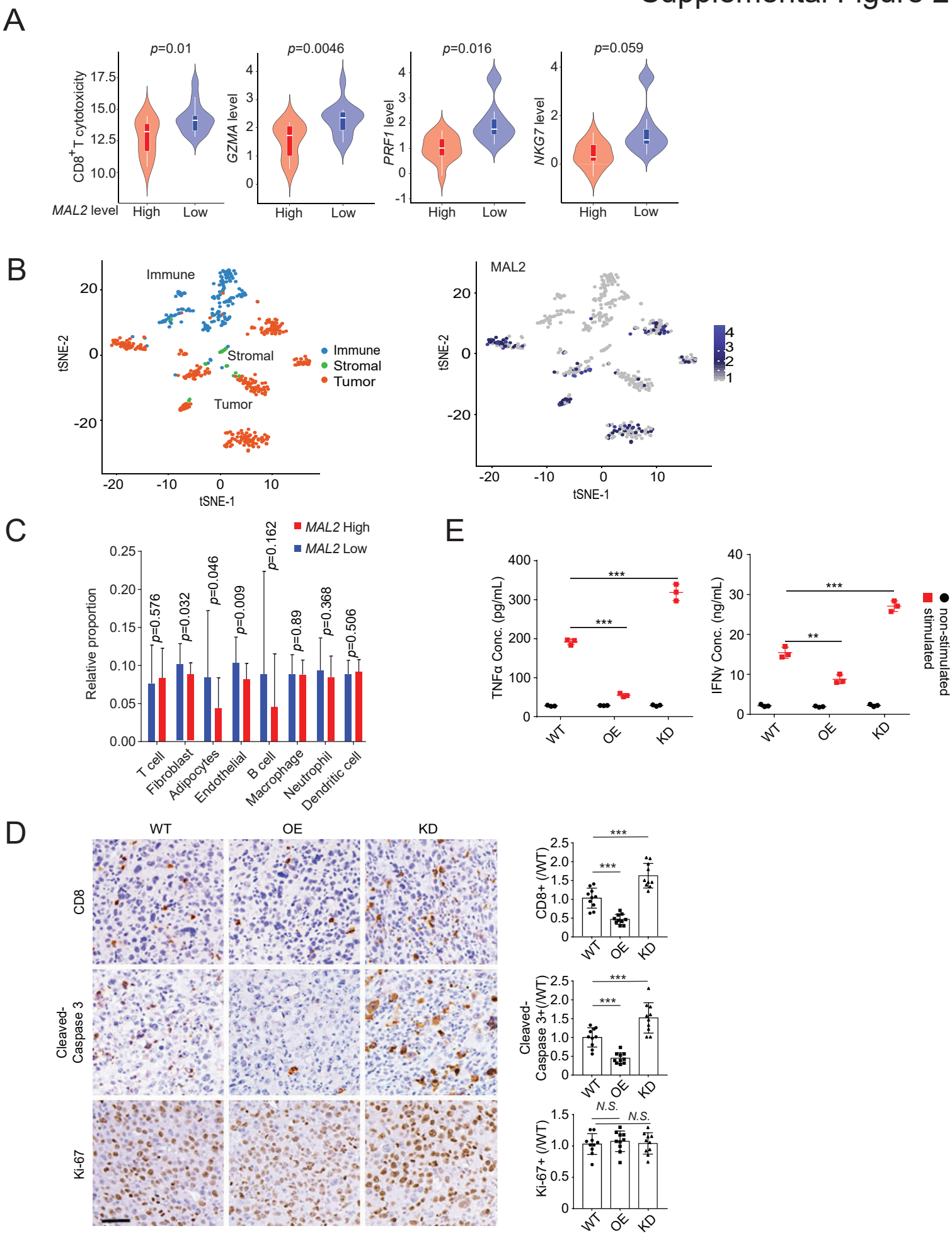

Supplemental Figure 2. MAL2 expression is correlated with low cytotoxicity of tumor-infiltrating CD8$^+$ T cells. (**A**) Violin plots representing Relative Cytotoxicity (RC) level of tumor-infiltrating CD8$^+$ T cells and normalized expression levels of 3 cytotoxic markers in TNBC samples with high or low Mal2 expression levels. The data of TNBC patients with high tumor infiltrating T cell levels are from GSE32646 cohort. Statistical analysis was conducted using unpaired 2-tailed t test. (**B**) t-SNE plot of 515 classified tumor and immune cells from 11 BRCA patients (scRNA-seq database GSE75688) indicates the distribution of MAL2-expressing cells. Immune cells, stromal cells and tumor cells are colored by cell types. Left panel, identifier; Right panel, MAL2 expression in different cell types. (**C**) Relative proportions of cell types in human TNBC tumor microenvironment. Bulk RNA-seq data of TNBC samples in TCGA was analyzed with Inference of cell types and deconvolution (ICTD). Two-way ANOVA test was used for statistical analysis. (**D**) Immunohistochemical (IHC) analysis (CD8, cleaved caspase-3 and Ki-67) of EO771 tumors in immunocompetent C57BL/6 mice. Representative IHC staining images are presented and quantitation results are mean± SD. Scale bar = 100 μm. Data are presented as mean ± SD. One-way ANOVA test was used for statistical analysis. (**E**) CD8$^+$ T cell isolated from 4T1 tumors in immunocompetent BALB/c mice were incubated with 50 ng/mL PMA for 5 hours, and supernatants were collected and tested by ELISA. TNFα and IFNγ levels are presented as mean ± SD of 3 individual tumors. Two-way ANOVA test was used for statistical analysis. *, $p<0.05$; **, $p<0.01$; ***, $p<0.001$; *N.S.*, no significance.

Supplemental Figure 3

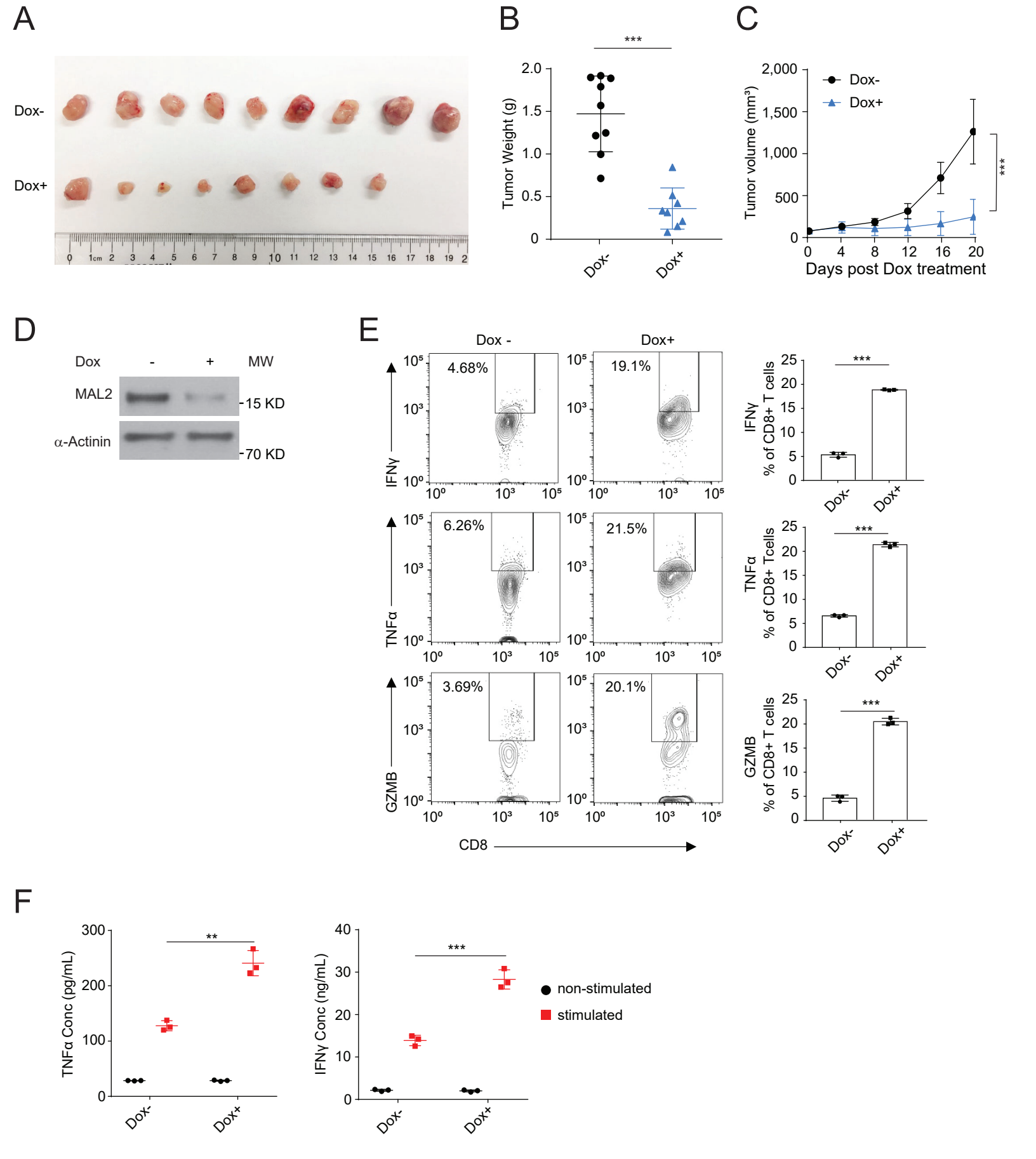

Supplemental Figure 3. Inducible MAL2 knockdown inhibits tumor growth by downregulating CD8$^+$ T cell activity. Dox-induced *Mal2* knockdown inhibits EO771 tumor growth in C57BL/6 mice. EO771 cells expressing Dox-inducible *Mal2* shRNA were orthotopically transplanted into 5-week-old female C57BL/6 mice (5 x 10^4 cells per mouse). Dox treatment was started through drinking water once the tumors were notable. Tumor size was monitored every 4 days. 20 days after the Dox treatment, mice were euthanized and the tumors were collected and weighted. Harvested tumors are shown in (**A**), tumor weight (**B**) and tumor growth (**C**) are quantitated. Data are presented as mean ± SD. One-way and two-way ANOVA tests were used for data analysis in tumor weight (B) and tumor growth (C), respectively. (**D**) Mal2 expression levels in EO771 tumors with or without Dox treatment. Immunoblotting of tissue lysates for MAL2 was applied and α-Actinin was used as loading control. (**E**) CD8$^+$ T cells were isolated from EO771 tumor tissues (Dox- vs Dox+) were analyzed by flow cytometry for their activity indicated by IFNγ, TNFα and GZMB levels in the cell. Flow cytometrical data are shown on the left and the quantitation results are summarized on the right. Two-way ANOVA test was used for statistical analysis. (**F**) CD8$^+$ T cells as above mentioned were analyzed for their secretion of cytokines (IFNγ, TNFα). Supernatants were collected and quantified by ELISA. Data are presented as mean ± SD. Two-way ANOVA test was used for statistical analysis. *, $p<0.05$; **, $p<0.01$; ***, $p<0.001$; *N.S.*, no significance.

Supplemental Figure 4

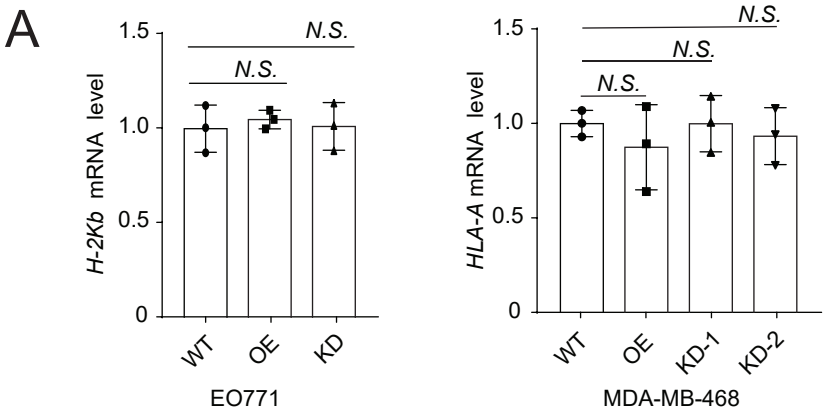

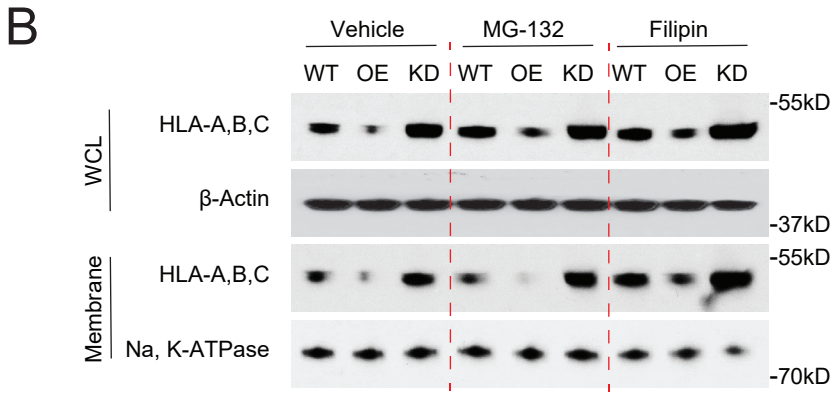

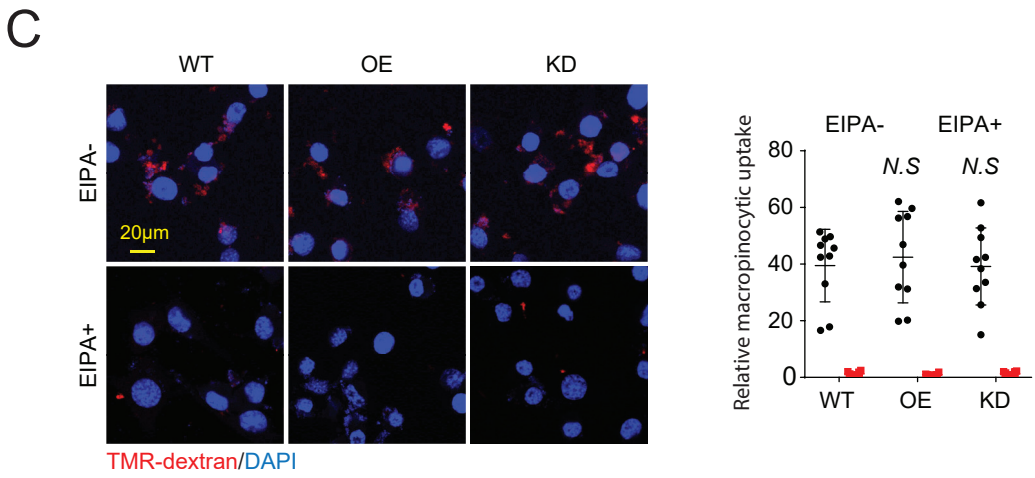

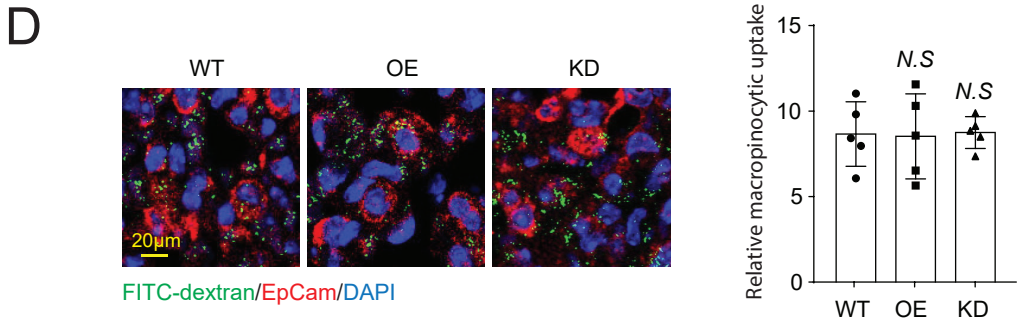

Supplemental Figure 4. MAL2 regulates the turnover of the MHC-I antigen presentation. (**A**) mRNA expression levels of MHC-I in EO771 (H-2Kb) and MDA-MB-468 (HLA-A) cells with different MAL2 expression levels. Quantitative PCR (qPCR) assay was applied and data are presented as mean ± SD of 3 independent experiments. Statistical analyses in the figure were conducted using one-way ANOVA test. *N.S.*, no significance. (**B**) MDA-MB-468 cells with different MAL2 levels were treated with proteasome inhibitor MG-132 or endocytosis inhibitor Filipin. Levels of MHC-I proteins (HLA-A, B, C) in the whole cell lysates and cell membrane fractions of MDA-MB-468 cells were determined by immunoblotting analyses (**C**) A macropinocytosis uptake assay using TMR-dextran as a marker of macropinosomes (red) indicates that MAL2 barely affects macropinocytosis in MDA-MB-468 cells. EIPA is an inhibitor for macropinocytosis. Scale bar is 20 μm. Data are presented as mean ± SD. *N.S.*, no significance. (**D**) Visualization and quantification of macropinocytosis in vivo. Representative images from sections of FITC-dextran (green)-injected EO771 tumors (in C57BL/6 mice) stained with anti-EpCAM (red). Scale bar is 20 μm. Data are presented as mean ± SD. *N.S.,* no significance.

Supplemental Figure 5

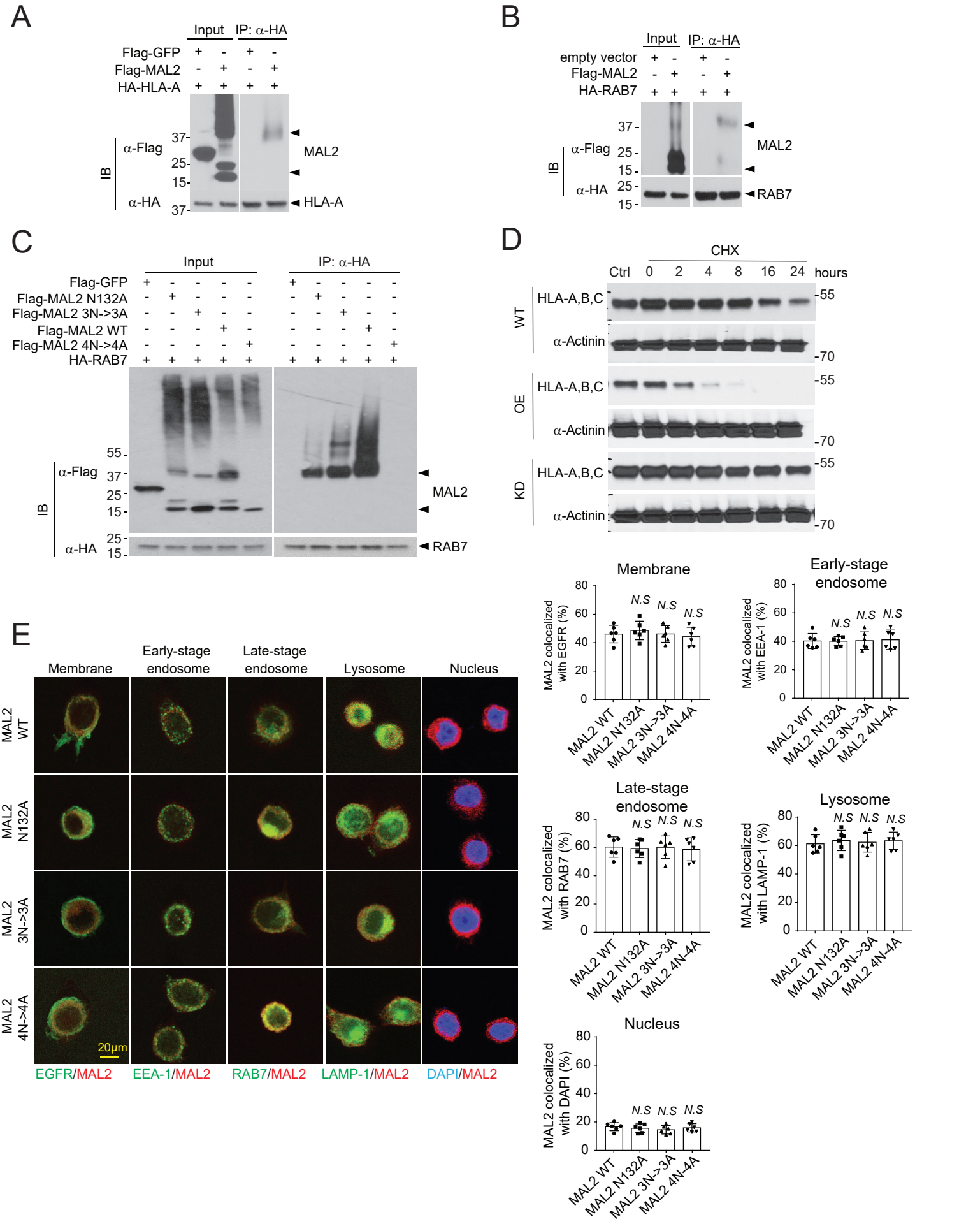

Supplemental Figure 5. MAL2 regulates the interaction of HLA with RAB7. (**A**) MAL2 is physically associated with HLA-A. Human MDA-MB-468 cells were transfected with Flag-tagged MAL2 and HA-tagged HLA-A2 (Flag-tagged GFP was used as negative control) and cell lysates were analyzed by co-immunoprecipitation (co-IP) and western blotting using indicated antibodies. (**B**) MAL2 is physically associated with RAB7. MDA-MB-468 cells expressing Flag-tagged MAL2 and HA-tagged RAB7 were analyzed as described in (A). (**C**) Glycosylation of MAL2 is essential for the interaction of MAL2 with RAB7. HA-tagged RAB7 and Flag-tagged full length or mutant MAL2 were co-expressed in human MDA-MB-468 cells. MAL2 was immunoprecipitated and the immunoprecipitates were analyzed by western blotting using indicated antibodies. Flag-tagged GFP was used as negative control. (**D**) MAL2 expression levels impact the half-life of endogenous HLA. MDA-MB-468 cells with different MAL2 expression levels (WT, OE and KD) were treated with 10 μg/mL cycloheximide (CHX) for 0-24 hours as indicated. Cells were then collected and lyzed, and immunoblotting was applied for detecting the level of HLA-A,B,C. α-Actinin served as loading control. (**E**) Localization of wildtype or glycosylation mutant MAL2 protein in MDA-MB-468 cells. EGFR is biomarker for membrane proteins. EEA-1 and RAB7 are biomarkers for early and late stage endosomes, respectively, and LAMP-1 is a biomarker for lysosomes. Colocalization is quantified by ImageJ. In this figure, data are presented as mean ± SD. *, $p<0.05$; **, $p<0.01$; ***, $p<0.001$; *N.S.*, no significance.

Supplemental Figure 6

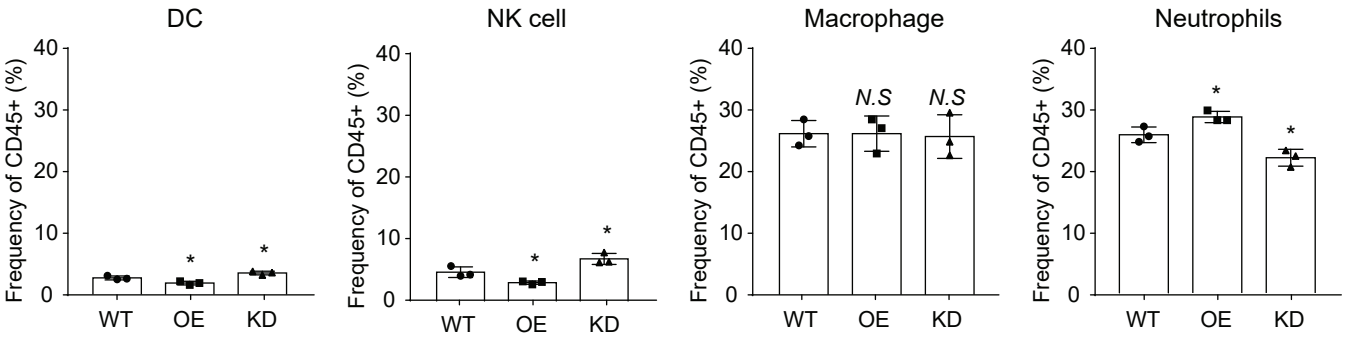

Supplemental Figure 6. MAL2 levels in EO771 tumors affect tumor-infiltration of innate immune cells. EO771 tumors were collected 21 days post-injection from C57BL/6 mice and digested into single cells. Infiltration of innate immune cells were analyzed using flow cytometry. Data are presented as mean ± SD. *, $p<0.05$; **, $p<0.01$; ***, $p<0.001$; N.S., no significance.

Supplemental Figure 7

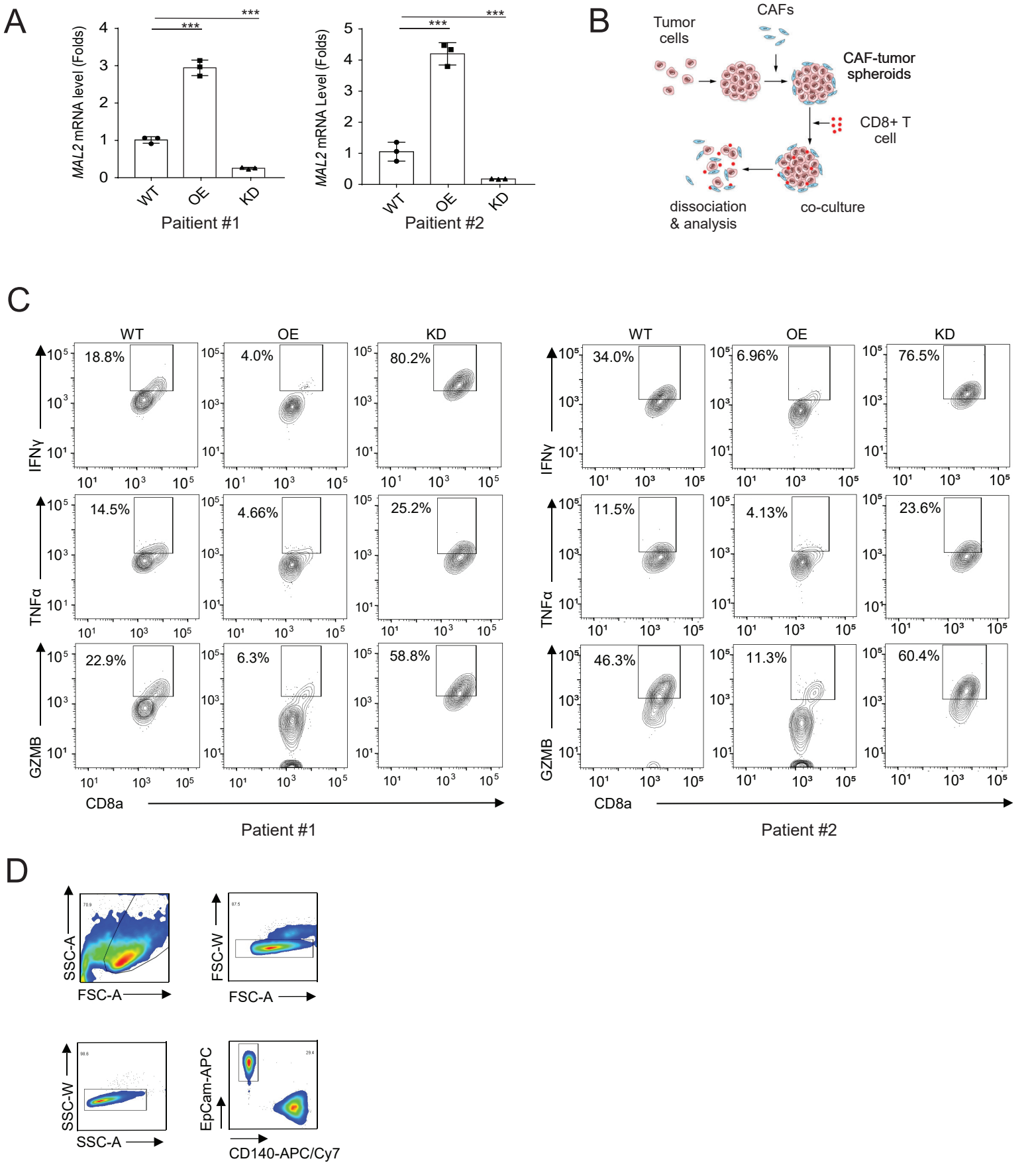

Supplemental Figure 7. MAL2 expressed in tumor cells regulates $CD8^+$ T cell cytotoxicity in human TNBC tumors. (**A**) *MAL2* mRNA expression levels in patient-derived tumor organoids with different *MAL2* expression levels (WT, OE and KD). Statistical analyses were conducted using one-way ANOVA test. Data are presented as mean ± SD. ***, $p<0.001$. (**B**) Flow chart illustrating the T cell cytotoxicity assay using patient-derived tumor organoids. (**C**) $CD8^+$ T cells isolated from the co-cultures of tumor organoids and $CD8^+$ T cells in (B) were analyzed by flow cytometry for their activity indicated by IFNγ, TNFα and GZMB levels in the cell. Flow cytometrical data are shown as represented. (**D**) Gating strategy for isolating tumor cells ($EpCAM^+/CD140^-$) from organoids.

Supplemental Figure 8

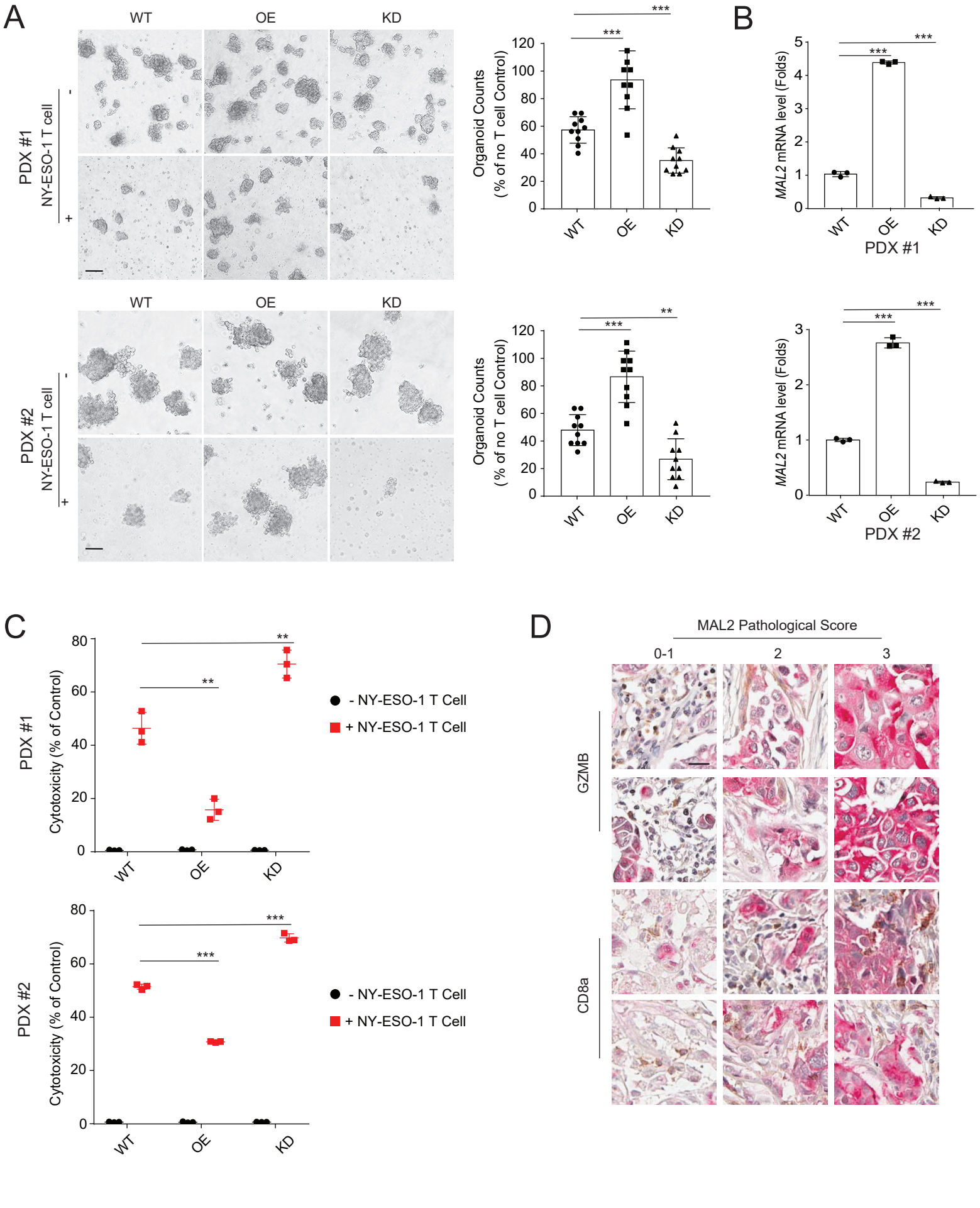

Supplemental Figure 8. MAL2 expressed in tumor cells regulates $CD8^+$ T cell cytotoxicity in PDX-derived tumor organoids. (**A**) NY-ESO-1-presenting human TNBC cells isolated from PDX tissues (PDX #1 and #2) were transduced with lentiviral MAL2 or its shRNA. The tumor cells formed CAF-tumor spheroids with matched mouse CAFs. When the majority diameters of spheroids reached 100 μm, the spheroids were co-cultured with pre-activated NY-ESO-1 specific $CD8^+$ T cell to assess T cell cytotoxicity (organoid dissociation rate). Images of spheroids (left panel) and quantitation (right panel) are shown as represented. Scale bar = 100 μm. Statistical analyses were conducted using one-way ANOVA test. Data are presented as mean ± SD. (**B**) *MAL2* mRNA expression levels were confirmed by qPCR assays in the PDX-generated spheroids with different Mal2 expression levels (WT, OE and KD). One-way ANOAVA test was used for statistical analysis. Data are presented as mean ± SD. (**C**) Flow cytometry analyses were conducted to determine the cytotoxicity of NY-ESO-1 specific CD8+ T cell cytotoxicity against PDX spheroids with different MAL2 expression levels (WT, OE and KD). Quantitation results are presented as mean ± SD of 3 parallel experiments. Two-way ANOAVA test was used for statistical analysis. Data are presented as mean ± SD. (**D**) Representative images from IHC staining of human breast cancer tissue microarrays. Mal2 is stained as red and the pathological scores for Mal2 staining intensity are shown, while GZMB and CD8a are stained separately as brown. Scale bar = 10 μm. *, $p<0.05$; **, $p<0.01$; ***, $p<0.001$.

Supplemental Table 1. Genes in TCR signaling pathways and patients sample ID for Figure 3C

Genes in TCR signaling pathway

No.	Gene	No.	Gene	No.	Gene	No.	Gene	No.	Gene
1	*CD1D*	51	*PHPT1*	101	*PELI1*	151	*CD46*	201	*XCL1*
2	*JAK3*	52	*MINK1*	102	*STAT5B*	152	*GIMAP5*	202	*ZP3*
3	*TNFAIP8L2*	53	*BTNL2*	103	*DUSP3*	153	*GATA3*	203	*FOXN1*
4	*CD209*	54	*AP3D1*	104	*SFTPD*	154	*NCK1*	204	*BCL11B*
5	*ADA*	55	*AP3B1*	105	*SPN*	155	*PYCARD*	205	*PDCD1*
6	*TNFSF11*	56	*BTN2A2*	106	*CDKN2A*	156	*TNFSF18*	206	*CCL21*
7	*IGF2*	57	*RPS6*	107	*IL12A*	157	*PTPN6*	207	*IL12RB1*
8	*TGFB1*	58	*B2M*	108	*PDCD1LG2*	158	*CXCL13*	208	*KCNN4*
9	*THY1*	59	*PDCD7*	109	*ABL2*	159	*IL1B*	209	*ITGAL*
10	*SPTA1*	60	*ABL1*	110	*TNFRSF14*	160	*IL7R*	210	*ZP4*
11	*AIF1*	61	*CD28*	111	*ITGB2*	161	*ZBTB16*	211	*CD3D*
12	*CD4*	62	*PDE5A*	112	*ZC3H8*	162	*PAWR*	212	*CACNA1F*
13	*GLI3*	63	*ITPKB*	113	*HSPH1*	163	*SOCS6*	213	*IL4*
14	*EFNB1*	64	*VSIG4*	114	*BCL10*	164	*ANXA1*	214	*HHLA2*
15	*LEF1*	65	*RPL22*	115	*CYLD*	165	*IL18*	215	*CCL19*
16	*CD300A*	66	*SATB1*	116	*TRAF2*	166	*EBI3*	216	*IL2RA*
17	*CD86*	67	*CARD11*	117	*ZBTB1*	167	*ELF1*	217	*IL36B*
18	*FAS*	68	*GPAM*	118	*PTPRJ*	168	*SIT1*	218	*VTCN1*
19	*TGFBR2*	69	*PRELID1*	119	*PTPN2*	169	*RAG1*	219	*CXCL10*
20	*LAT*	70	*CTNNB1*	120	*SLC46A2*	170	*IL27*	220	*IFNA2*
21	*NCKAP1L*	71	*HES1*	121	*SIVA1*	171	*CD274*	221	*ICOSLG*
22	*CD276*	72	*SRF*	122	*RIPK2*	172	*SYK*	222	*SIRPG*
23	*ZEB1*	73	*ADAM10*	123	*IHH*	173	*CD24*	223	*LGALS16*
24	*LAG3*	74	*NCK2*	124	*STX7*	174	*LILRB1*	224	*IL2*
25	*VCAM1*	75	*CASP3*	125	*ITGAM*	175	*CCL5*	225	*LCK*
26	*CORO1A*	76	*MALT1*	126	*IL23A*	176	*P2RX7*	226	*TIGIT*
27	*ZNHIT1*	77	*SOD1*	127	*BLM*	177	*CD80*	227	*LGALS14*
28	*SPINK5*	78	*AKT1*	128	*ADK*	178	*CCL2*	228	*CCR7*
29	*PTPN22*	79	*MYH9*	129	*PTPRC*	179	*TMEM102*	229	*IFNB1*
30	*EGR3*	80	*IL10*	130	*ADAM17*	180	*IFNL1*	230	*AZGP1*
31	*CBLB*	81	*DHPS*	131	*DOCK8*	181	*IL6*	231	*LGALS13*
32	*BTN3A1*	82	*GLMN*	132	*CD59*	182	*PRKCQ*	232	*IL12B*
33	*PRKD2*	83	*PAX1*	133	*LRRC32*	183	*IL23R*	233	*SHH*
34	*CADM1*	84	*CLPTM1*	134	*GBP1*	184	*HFE*	234	*IL1RL2*
35	*WNT5A*	85	*NKAP*	135	*SIGLEC1*	185	*IL20RB*	235	*IFNL3*
36	*GLI2*	86	*NDFIP1*	136	*PNP*	186	*DTX1*	236	*CD247*
37	*FYN*	87	*MAP3K7*	137	*CTLA4*	187	*IGF1*	237	*UBASH3A*

38	*CAMK4*	88	*IL7*	138	*TRAF6*	188	*PIP*	238	*CD3E*
39	*CD74*	89	*CD27*	139	*STAT5A*	189	*IFNL2*	239	*FOXJ1*
40	*BMP4*	90	*SASH3*	140	*CD47*	190	*IKZF1*	240	*TESPA1*
41	*TCF7*	91	*BRAF*	141	*PAG1*	191	*TNFSF13B*	241	*IL21*
42	*MR1*	92	*FADD*	142	*CEBPB*	192	*RSAD2*	242	*TNFSF14*
43	*STK11*	93	*PRNP*	143	*BAD*	193	*IL15*	243	*CCL20*
44	*IL6ST*	94	*TNFRSF13C*	144	*FOXP3*	194	*VNN1*	244	*IFNG*
45	*IGFBP2*	95	*RC3H1*	145	*LGALS3*	195	*NKX2-3*	245	*TRAT1*
46	*TNFSF4*	96	*KIAA0922*	146	*ERBB2*	196	*ZAP70*	246	*CD2*
47	*CXCL12*	97	*DOCK2*	147	*LILRB2*	197	*TMIGD2*	247	*IDO1*
48	*ADAM8*	98	*DLG1*	148	*ITGAD*	198	*SCGB1A1*	248	*LAX1*
49	*TNFRSF21*	99	*DNAJA3*	149	*TNFSF9*	199	*S100A7*	249	*CCR2*
50	*FZD5*	100	*NFKBID*	150	*NRARP*	200	*CRTAM*	250	*CD3G*

Patient sample ID

No.	Patient sample ID	No.	Patient sample ID	No.	Patient sample ID	No.	Patient sample ID
1	TCGA_AC_A2QH	30	TCGA_A2_A1G6	59	TCGA_D8_A1JF	88	TCGA_AC_A6IW
2	TCGA_AC_A7VC	31	TCGA_C8_A131	60	TCGA_AN_A0XU	89	TCGA_LL_A441
3	TCGA_AO_A12F	32	TCGA_AO_A124	61	TCGA_A2_A3XY	90	TCGA_E2_A14X
4	TCGA_AN_A04D	33	TCGA_EW_A1P8	62	TCGA_BH_A0B3	91	TCGA_AO_A0J4
5	TCGA_AR_A2LR	34	TCGA_EW_A1PH	63	TCGA_AR_A1AR	92	TCGA_GM_A2DB
6	TCGA_AR_A1AY	35	TCGA_A2_A0T2	64	TCGA_AR_A5QQ	93	TCGA_A2_A0CM
7	TCGA_AC_A2QJ	36	TCGA_BH_A18V	65	TCGA_GM_A2DF	94	TCGA_AR_A0TU
8	TCGA_E9_A5FL	37	TCGA_A2_A0T0	66	TCGA_D8_A1XK	95	TCGA_AO_A1KR
9	TCGA_A1_A0SK	38	TCGA_D8_A13Z	67	TCGA_BH_A0E0	96	TCGA_HN_A2NL
10	TCGA_GI_A2C9	39	TCGA_C8_A1HJ	68	TCGA_BH_A42U	97	TCGA_E2_A14R
11	TCGA_D8_A27F	40	TCGA_BH_A0WA	69	TCGA_D8_A27M	98	TCGA_A8_A09X
12	TCGA_A2_A0YE	41	TCGA_B6_A400	70	TCGA_A7_A6VY	99	TCGA_BH_A0BG
13	TCGA_E2_A1LL	42	TCGA_A1_A0SP	71	TCGA_A8_A08R	100	TCGA_C8_A12V
14	TCGA_AO_A0JL	43	TCGA_AR_A0U4	72	TCGA_D8_A1XQ	101	TCGA_E2_A14N
15	TCGA_D8_A27H	44	TCGA_E2_A158	73	TCGA_LL_A73Y	102	TCGA_AO_A129
16	TCGA_A2_A04U	45	TCGA_BH_A1EW	74	TCGA_D8_A1JL	103	TCGA_E2_A1LH
17	TCGA_A7_A0DA	46	TCGA_C8_A3M7	75	TCGA_C8_A26X	104	TCGA_S3_AA10
18	TCGA_B6_A402	47	TCGA_A2_A3XT	76	TCGA_EW_A1P4	105	TCGA_EW_A1PB
19	TCGA_A7_A6VW	48	TCGA_BH_A0BL	77	TCGA_D8_A147	106	TCGA_EW_A1OV
20	TCGA_A7_A4SE	49	TCGA_C8_A26Y	78	TCGA_AQ_A04J	107	TCGA_GM_A2DH
21	TCGA_E2_A1LS	50	TCGA_E2_A150	79	TCGA_AN_A0AT	108	TCGA_LL_A5YO
22	TCGA_AO_A03U	51	TCGA_S3_AA15	80	TCGA_E2_A1L7	109	TCGA_AO_A0J6
23	TCGA_EW_A1OW	52	TCGA_BH_A1F6	81	TCGA_BH_A0RX	110	TCGA_B6_A3ZX
24	TCGA_AN_A0AR	53	TCGA_AN_A0AL	82	TCGA_EW_A3U0	111	TCGA_BH_A0B9
25	TCGA_AC_A2BK	54	TCGA_A2_A3XX	83	TCGA_AR_A0TS	112	TCGA_BH_A1FC
26	TCGA_AR_A256	55	TCGA_A7_A26G	84	TCGA_A2_A0D2	113	TCGA_C8_A27B
27	TCGA_AN_A0G0	56	TCGA_OL_A6VO	85	TCGA_A2_A0SX	114	TCGA_AO_A128
28	TCGA_A7_A6VV	57	TCGA_D8_A143	86	TCGA_A2_A0D0	115	TCGA_EW_A6SB
29	TCGA_BH_A18G	58	TCGA_A8_A07O	87	TCGA_A8_A07C		

Supplemental Table 2. Proteins identified as potential MAL2 interactors from mass spectrometry for Figure 5A.

Protein	p-value	Protein	p-value	Protein	p-value	Protein	p-value	Protein	p-value
OST48	< 0.00010	GPAT4	< 0.00010	FUBP1	0.0036	STX3	0.0067	PLIN3	0.024
H90B3	< 0.00010	H90B4	< 0.00010	G3P	0.0036	TPP1	0.0067	SYFA	0.024
AT5F1	< 0.00010	UBB	< 0.00010	HAX1	0.0036	B4DLN1	0.0067	PTSS2	0.024
RB11B	< 0.00010	ARF4	0.00016	1A68	0.0036	1433B	0.013	SAAL1	0.024
RAB1A	< 0.00010	AGK	0.00016	HS105	0.0036	1433G	0.013	YIPF3	0.024
TFR1	< 0.00010	NP1L1	0.00016	ENPL	0.0036	CCD47	0.013	RABL3	0.024
RB11A	< 0.00010	ECM29	0.00016	HS905	0.0036	CYTSA	0.013	RAB5B	0.024
ATP5H	< 0.00010	RAB8A	0.00016	HAT1	0.0036	DNJA3	0.013	VAT1	0.024
RAB1B	< 0.00010	STIP1	0.00016	PCAT1	0.0036	DPM1	0.013	TTC4	0.024
GRP75	< 0.00010	FANCI	0.00029	MSPD2	0.0036	FAS	0.013	VATH	0.024
HLAA	< 0.00010	MYL6	0.00029	PCBP2	0.0036	SAR1A	0.013	COPB2	0.044
DYHC1	< 0.00010	NUP93	0.00029	RUVB1	0.0036	GCDH	0.013	EXOC7	0.044
STT3A	< 0.00010	ILVBL	0.00055	AT1B3	0.0036	LMNB1	0.013	FACR1	0.044
RAB7A	< 0.00010	CHP1	0.00055	SMC4	0.0036	MBOA7	0.013	QPCT	0.044
B4GA1	< 0.00010	LTN1	0.00055	ECHB	0.0036	MIC13	0.013	GOGA5	0.044
HLAB	< 0.00010	NB5R3	0.00055	TBAL3	0.0036	MYH14	0.013	HLAE	0.044
PSA	< 0.00010	SURF4	0.00055	DESM	0.0036	NOMO2	0.013	HLAH	0.044
ATPG	< 0.00010	RHOA	0.00055	ATPD	0.0067	TBRG4	0.013	S27A4	0.044
ESYT1	< 0.00010	TM9S3	0.00055	NTPCR	0.0067	SPNS1	0.013	MRS2	0.044
MYH11	< 0.00010	ARF5	0.001	ALG1	0.0067	K7ERQ8	0.013	PGRC2	0.044
VATA	< 0.00010	BZW2	0.001	CLH1	0.0067	RAB6B	0.013	MYL6B	0.044
ATP5L	< 0.00010	FUBP2	0.001	COPA	0.0067	RB39B	0.013	NDUS8	0.044
COX15	< 0.00010	GANAB	0.001	CND1	0.0067	RCN1	0.013	CN37	0.044
DNJA2	< 0.00010	PARP1	0.001	DHC24	0.0067	AT2A3	0.013	CDS2	0.044
TIM50	< 0.00010	YIF1B	0.001	EFHD2	0.0067	SCAM2	0.013	SAC1	0.044
RFIP1	< 0.00010	RAB14	0.001	RAN	0.0067	SRPRB	0.013	UN45A	0.044
CERS2	< 0.00010	SCAM3	0.001	H4	0.0067	TIF1B	0.013	LTOR1	0.044
DAAF5	< 0.00010	TCPZ	0.001	CP51A	0.0067	TMED2	0.013	RAB2B	0.044
RAB35	< 0.00010	DHB12	0.001	MLEC	0.0067	AR6P1	0.024	RAB37	0.044
HLAC	< 0.00010	AUP1	0.0019	SYMC	0.0067	APMAP	0.024	RAB12	0.044
TNPO1	< 0.00010	COX5A	0.0019	TIM44	0.0067	CLPT1	0.024	RACK1	0.044
HACD3	< 0.00010	EMD	0.0019	TIM23	0.0067	CLP1L	0.024	RDH11	0.044
ARF1	< 0.00010	FAF2	0.0019	AAAT	0.0067	DDRGK	0.024	SPTC1	0.044
H90B2	< 0.00010	HS904	0.0019	PRAF3	0.0067	DRS7B	0.024	2AAB	0.044
S61A1	< 0.00010	HMOX1	0.0019	S61A2	0.0067	ALG5	0.024	ATP4A	0.044
2AAA	< 0.00010	PCBP1	0.0019	RAB2A	0.0067	1B73	0.024	TELO2	0.044
PTN1	< 0.00010	TBRG1	0.0019	RAB6A	0.0067	MOFA1	0.024	SEC63	0.044
LMAN2	< 0.00010	SC22B	0.0019	RAB3A	0.0067	MIRO2	0.024	UBQL1	0.044

ATP5J	< 0.00010	PRS6A	0.0036	RB39A	0.0067	MBB1A	0.024
MCM3	< 0.00010	PRS10	0.0036	SMC2	0.0067	NCLN	0.024

Supplemental Table 3. Selected gene markers for CD3$^+$ T cell clustering for Figure 8A.

Gene	Cluster	p-value	Average log fold change
Ms4a4b	Cd8 Effector	5.21E-240	0.32635203
Nkg7	Cd8 Effector	1.86E-137	0.248487373
Rps27	Cd8 Effector	8.70E-121	0.184266692
Ms4a6b	Cd8 Effector	3.84E-108	0.188708833
Pdcd4	Cd8 Effector	2.70E-99	0.188009158
Mndal	Cd8 Effector	6.38E-95	0.17265192
Ltb	Cd8 Effector	8.90E-89	0.169262847
Arl4c	Cd8 Effector	7.85E-79	0.196159876
Epsti1	Cd8 Effector	1.75E-73	0.167795973
Bcl2	Cd8 Effector	1.33E-69	0.197477349
Cd8b1	Cd8 Effector	3.23E-67	0.228537587
Cd8a	Cd8 Effector	2.88E-65	0.181698646
Ly6c2	Cd8 Effector	3.70E-59	0.287888123
Plac8	Cd8 Effector	1.84E-56	0.256715505
Hcst	Cd8 Effector	5.26E-48	0.170494919
Klrd1	Cd8 Effector	5.89E-47	0.191092664
Klf2	Cd8 Effector	8.26E-28	0.206157059
Igkc	Cd8 Effector	1.23E-25	0.218942069
Ccl5	Cd8 Effector	6.89E-25	0.208765277
Il7r	Cd8 Effector	5.19E-13	0.16551623
Igkc	Cd8 Naive I	0	0.583515716
Malat1	Cd8 Naive I	0	0.560665467
Rps27	Cd8 Naive I	0	0.440830036
Btg1	Cd8 Naive I	8.35E-264	0.52828201
Klf2	Cd8 Naive I	4.46E-243	0.638133029
Arhgap45	Cd8 Naive I	8.64E-226	0.487345966
Ms4a4b	Cd8 Naive I	2.45E-222	0.479070374
Igha	Cd8 Naive I	2.28E-201	0.397214137
Mbnl1	Cd8 Naive I	6.80E-190	0.415603059
Ifi203	Cd8 Naive I	1.60E-188	0.457771817
S1pr1	Cd8 Naive I	4.43E-182	0.438573061
mt-Nd4l	Cd8 Naive I	2.23E-170	0.419938599
Selenow	Cd8 Naive I	2.87E-160	0.402226411
Rsrp1	Cd8 Naive I	8.79E-143	0.396397946
Txnip	Cd8 Naive I	2.29E-132	0.434670952
Hcst	Cd8 Naive I	3.92E-127	0.41411096
Il7r	Cd8 Naive I	8.66E-122	0.553356997
Arhgap15	Cd8 Naive I	8.74E-121	4.05E-01
S100a4	Cd8 Naive I	1.06E-35	4.06E-01
Ccl5	Cd8 Naive I	2.72E-27	5.89E-01

Pkm	Cd8 Naive II	1.84E-178	0.487655866
Gapdh	Cd8 Naive II	2.96E-168	0.426636145
Tpi1	Cd8 Naive II	1.50E-157	0.525441306
Ldha	Cd8 Naive II	3.15E-156	0.454476303
Tnfrsf4	Cd8 Naive II	1.27E-145	0.64933652
Pgk1	Cd8 Naive II	1.30E-142	0.435322784
Aldoa	Cd8 Naive II	4.20E-139	0.381842718
Mif	Cd8 Naive II	5.79E-136	0.414504123
Pgam1	Cd8 Naive II	2.71E-132	0.396842247
Pla2g12a	Cd8 Naive II	5.03E-119	0.392244879
Hsp90aa1	Cd8 Naive II	1.21E-108	0.358611615
Odc1	Cd8 Naive II	6.84E-104	0.416298434
Sub1	Cd8 Naive II	1.25E-93	0.376620777
Il2ra	Cd8 Naive II	8.96E-92	0.372317362
Sdf4	Cd8 Naive II	1.80E-88	0.404900986
Srgn	Cd8 Naive II	1.46E-87	0.39136131
Batf	Cd8 Naive II	1.35E-74	0.354641809
Tnfrsf9	Cd8 Naive II	2.93E-52	0.445160497
Ccl4	Cd8 Naive II	4.50E-20	0.781412015
Ifng	Cd8 Naive II	0.001324061	0.357654855
Pkm	NKT	1.76E-288	0.533496228
Gapdh	NKT	5.04E-270	0.459444671
Ldha	NKT	1.25E-255	0.490310416
Tpi1	NKT	5.52E-239	0.550662246
Pgk1	NKT	1.01E-222	0.465093447
Tnfrsf4	NKT	5.09E-209	0.657788309
Mif	NKT	2.78E-203	0.428770306
Aldoa	NKT	5.80E-195	0.382360504
Pgam1	NKT	1.03E-180	0.392828415
Eno1	NKT	3.91E-171	0.369319454
Hsp90aa1	NKT	9.48E-169	3.77E-01
Il2ra	NKT	1.60E-157	4.02E-01
Odc1	NKT	4.86E-157	4.23E-01
Sub1	NKT	1.44E-143	4.02E-01
Batf	NKT	8.38E-130	3.80E-01
Srgn	NKT	4.08E-122	3.62E-01
Sdf4	NKT	1.66E-121	3.93E-01
Tnfrsf18	NKT	4.06E-118	3.83E-01
Ly6a	NKT	3.98E-103	3.77E-01
Tnfrsf9	NKT	1.05E-65	4.68E-01
Pkm	CD4 Naive	1.02E-207	0.512098244
Gapdh	CD4 Naive	7.82E-188	0.431149936
Ldha	CD4 Naive	1.56E-184	0.471694405
Tpi1	CD4 Naive	1.30E-172	0.510949274

Tnfrsf4	CD4 Naive	1.25E-167	0.663275537
Pgk1	CD4 Naive	6.21E-159	0.441892791
Aldoa	CD4 Naive	1.08E-151	0.3777668
Mif	CD4 Naive	2.35E-148	0.406069267
Pgam1	CD4 Naive	2.47E-145	0.393184809
Hsp90aa1	CD4 Naive	1.36E-122	0.360225275
Pla2g12a	CD4 Naive	3.25E-121	0.355161246
Sub1	CD4 Naive	9.78E-110	4.01E-01
Il2ra	CD4 Naive	1.73E-108	3.79E-01
Odc1	CD4 Naive	3.33E-108	3.91E-01
Srgn	CD4 Naive	6.35E-97	4.04E-01
Sdf4	CD4 Naive	4.38E-88	3.66E-01
Ly6a	CD4 Naive	9.67E-76	3.55E-01
Tnfrsf9	CD4 Naive	3.78E-50	4.30E-01
Ccl4	CD4 Naive	9.44E-36	4.68E-01
Ccl3	CD4 Naive	0.006164797	4.80E-01
Pkm	Tem	4.17E-227	0.499475257
Gapdh	Tem	7.98E-211	0.430019235
Ldha	Tem	5.70E-193	0.451757471
Tpi1	Tem	2.98E-185	0.507692774
Pgk1	Tem	2.06E-170	0.42725995
Mif	Tem	1.95E-169	0.408805113
Pgam1	Tem	2.71E-163	0.394518247
Tnfrsf4	Tem	2.53E-152	0.610373584
Hsp90aa1	Tem	4.12E-151	0.376161089
Pla2g12a	Tem	3.50E-150	0.384190594
Aldoa	Tem	1.13E-146	0.354558372
Eno1	Tem	2.28E-141	0.350875743
Fabp5	Tem	8.00E-132	0.341967744
Sub1	Tem	1.39E-127	0.379305658
Odc1	Tem	1.80E-118	0.373521918
Hspd1	Tem	1.06E-107	3.44E-01
Srgn	Tem	1.45E-99	3.63E-01
Sdf4	Tem	1.23E-81	3.47E-01
Ly6a	Tem	4.17E-77	3.38E-01
Tnfrsf9	Tem	6.46E-55	3.50E-01
Ms4a4b	Th1	4.43E-76	0.208659188
Nkg7	Th1	4.72E-75	0.187991974
Cd8a	Th1	1.50E-57	0.200719853
Ms4a4c	Th1	1.06E-49	0.137244286
Gm47283	Th1	1.83E-47	0.126948307
Cd8b1	Th1	1.80E-43	0.193638604
Bcl2	Th1	2.10E-40	0.178030178
Ctsw	Th1	3.01E-40	0.119306354

Ly6c2	Th1	1.66E-37	0.266532714
Plac8	Th1	1.82E-36	0.247585436
Arl4c	Th1	8.74E-35	1.38E-01
Pdcd4	Th1	3.31E-34	1.33E-01
Ms4a6b	Th1	7.68E-33	1.31E-01
Grap2	Th1	1.13E-30	1.13E-01
Thy1	Th1	9.37E-30	1.35E-01
Sell	Th1	2.12E-21	1.16E-01
Cdk6	Th1	1.38E-17	1.33E-01
Ccr7	Th1	1.11E-16	1.25E-01
Trdc	Th1	1.19E-07	1.30E-01
Xcl1	Th1	6.06E-05	1.64E-01
Tpi1	Th2	0	0.541884922
Pkm	Th2	0	0.537737235
Ldha	Th2	0	0.488801079
Gapdh	Th2	0	0.456086956
Tnfrsf4	Th2	5.90E-306	0.723217633
Pgk1	Th2	2.19E-298	0.461084553
Mif	Th2	8.81E-283	0.434472128
Pgam1	Th2	5.81E-265	4.13E-01
Aldoa	Th2	1.19E-263	3.86E-01
Pla2g12a	Th2	8.94E-244	4.04E-01
Hsp90aa1	Th2	1.21E-237	3.94E-01
Il2ra	Th2	6.73E-218	4.29E-01
Sub1	Th2	1.26E-209	4.34E-01
Odc1	Th2	1.41E-203	4.12E-01
Srgn	Th2	5.53E-187	4.35E-01
Sdf4	Th2	1.71E-177	4.25E-01
Ly6a	Th2	7.67E-163	4.30E-01
Tnfrsf18	Th2	1.33E-157	3.88E-01
Tnfrsf9	Th2	2.33E-94	4.62E-01
Ccl4	Th2	7.51E-90	4.86E-01
Ms4a4b	Treg	6.06E-94	0.305640295
Rps27	Treg	1.09E-83	0.238708233
Malat1	Treg	1.51E-70	0.297906138
Ms4a6b	Treg	3.72E-60	0.237888566
Ltb	Treg	7.60E-56	2.20E-01
Igkc	Treg	1.28E-52	2.84E-01
Mbnl1	Treg	4.57E-50	2.11E-01
Arhgap45	Treg	2.54E-49	2.56E-01
Btg1	Treg	4.99E-45	3.02E-01
Pdcd4	Treg	1.67E-43	2.25E-01
Selenow	Treg	6.83E-38	2.08E-01
Klf2	Treg	4.61E-35	3.31E-01

Hcst	Treg	4.07E-30	2.20E-01
Txnip	Treg	2.14E-23	2.13E-01
Clk1	Treg	6.59E-20	2.04E-01
Il7r	Treg	2.65E-12	2.89E-01
Hspa1b	Treg	1.54E-10	2.05E-01
Ly6c2	Treg	5.97E-08	2.08E-01
Ccl5	Treg	1.33E-05	3.05E-01
Trdc	Treg	1.56E-05	2.41E-01
Rps27	Tscm	3.90E-74	0.348987588
Igkc	Tscm	3.21E-72	0.442473476
Malat1	Tscm	5.90E-63	0.418475663
Ms4a4b	Tscm	1.50E-54	0.388580811
Mbnl1	Tscm	3.72E-50	0.348701688
Arhgap45	Tscm	2.89E-48	0.395994493
Btg1	Tscm	3.28E-45	0.407657753
mt-Nd4l	Tscm	1.14E-42	0.363429961
Klf2	Tscm	1.22E-39	0.415255311
Selenow	Tscm	5.84E-35	0.323176884
Gm2682	Tscm	9.33E-34	0.319328248
Txnip	Tscm	2.96E-29	0.346566861
Hcst	Tscm	8.28E-29	0.343182435
Adgre5	Tscm	7.85E-28	0.323249287
Il7r	Tscm	1.18E-26	0.506476492
Arl4c	Tscm	1.52E-22	0.308283562
Tsc22d3	Tscm	2.19E-16	0.309256439
Ccl5	Tscm	1.55E-13	4.99E-01
S100a6	Tscm	6.61E-11	3.73E-01
S100a4	Tscm	2.01E-09	3.11E-01

Supplemental Table 4. MAL2 and GZMB reads and scores in breast tumor tissue microarray analysis for Figure 9E.

BC081120e

	1	2	3	4	5	6	7	8	9	10	
A	**IDC**	**IDC**	**IDC**	**IDC**	**IDC**	**IDC**	**IDC**	**IDC**	**IDC**	**IDC**	
	T2N0M0	T2N0M0	T2N0M0	T2N1M0	T1N0M0	T1N0M0	T2N1M0	T2N0M0	T2N0M0	T2N0M0	
	TORN	+/-	+/-	3	+/-	1	Neg	1	Neg	2	**MAL2 Score**
		0.2870	0.0782	0.5172	0.0343	0.1345	0.0394	0.1444	0.0563	0.26391	**MAL2 Reads**
		0.0126	0.0090	0.0064	0.0090	0.0136	0.0106	0.0222	0.0114	0.0303	**GZMB Reads**
B	**IDC**	**IDC**	**IDC**	**IDC**	**IDC**	**IDC**	**IDC**	**IDC**	**IDC**	**IDC**	
	T1N1M0	T2N1M0	T2N0M0	T2N0M0	T2N0M0	T1N1M0	T2N0M0	T4N0M0	T2N0M0	T3N1M0	
	TORN	Neg	MISSING	+/-	S/F/M	1	2	3	3	3	**MAL2 Score**
		0.0810		0.1819		0.2498	0.3352	0.4883	0.5054	0.5840	**MAL2 Reads**
		0.0260		0.0130		0.0093	0.0079	0.0061	0.0091	0.0112	**GZMB Reads**
C	**IDC**	**IDC**	**IDC**	**IDC**	**IDC**	**IDC**	**IDC**	**IDC**	**IDC**	**IDC**	
	T2N1M0	T2N0M0	T2N0M0	T2N0M0	T2N0M0	T2N1M0	T2N0M0	T2N0M0	T2N0M0	T2N0M0	
	+/-	+/-	+/-	+/-	TORN	TORN	Neg	+/-	+/-	Neg	**MAL2 Score**
	0.1163	0.2519	0.0472	0.3153			0.1028	0.2160	0.3856	0.2104	**MAL2 Reads**
	0.0206	0.0148	0.0100	0.0097			0.0142	0.0101	0.0155	0.0041	**GZMB Reads**
D	**IDC**	**IDC**	**IDC**	**IDC**	**IDC**	**IDC**	**IDC**	**IDC**	**IDC**	**Intraductal Ca.**	
	T3N0M0	T2N0M0	T2N1M0	T3N2M0	T3N0M0	T2N0M0	T2N0M0	T2N1M0	T3N0M0	T3N0M0	
	+/-	1	Neg	+/-	+/-	1	Neg	1	+/-	1	**MAL2 Score**
	0.2897	0.2755	0.0230	0.3268	0.2776	0.1648	0.0030	0.5118	0.2366	0.2609	**MAL2 Reads**
	0.0267	0.0122	0.0040	0.0074	0.0108	0.0173	0.0112	0.0062	0.0136	0.0131	**GZMB Reads**
E	**IDC**	**IDC**	**IDC**	**IDC**	**IDC**	**IDC**	**IDC**	**IDC**	**IDC**	**IDC**	
	T3N0M0	T3N0M0	T4N2M0	T2N1M0	T2N1M0	T2N1M0	T2N0M0	T1N0M0	T2N1M0	T3N1M0	
	Neg	1	1	2	+/-	1	2	1	1	2	**MAL2 Score**
	0.1594	0.2457	0.2584	0.3356	0.1764	0.1377	0.2477	0.2589	0.2292	0.2901	**MAL2 Reads**
	0.0185	0.0136	0.0118	0.0098	0.0148	0.0151	0.0086	0.0171	0.0076	0.0040	**GZMB Reads**

F	IDC	IDC	IDC	IDC	IDC	IDC	IDC	IDC	IDC	IDC	
	T2N2M0	T2N2M0	T4N2M0	T2N0M0	T4N0M0	T3N0M0	T4N1M0	T4N1M0	T2N0M0	T1CN0M0	
	+/-	+/-	3	+/-	+/-	Neg	2	1	3	Neg	**MAL2 Score**
	0.1043	0.3529	0.1374	0.1026	0.0704	0.0568	0.2411	0.1856	0.7162	0.0215	**MAL2 Reads**
	0.0190	0.0169	0.0100	0.0247	0.0189	0.0161	0.0098	0.0252	0.0026	0.0451	**GZMB Reads**
G	**IDC**	**IDC**	**IDC**	**IDC**	**IDC**	**IDC**	**IDC**	**IDC**	**IDC**	**IDC**	
	T1N0M0	T2N0M0	T2N1M0	T2N0M0	T2N0M0	T3N1M0	T2N1M0	T4N2M0	T3N1M0	T2N0M0	
	2	2	TORN	S/F/M	2	Neg	+/-	+/-	Neg	3	**MAL2 Score**
	0.2653	0.3051			0.2103	0.1321	0.1409	0.1832	0.0460	0.4203	**MAL2 Reads**
	0.0196	0.0127			0.0059	0.0101	0.0109	0.0136	0.0174	0.0093	**GZMB Reads**
H	**IDC**	**IDC**	**IDC**	**IDC**	**IDC**	**IDC**	**IDC**	**IDC**	**IDC**	**IDC**	
	T2N1M0	T2N0M0	T1N0M0	T3N2M0	T2N2M0	T2N0M0	T2N0M0	T2N0M0	T4CN2M0	T4N0M0	
	2	+/-	+/-	Neg	2	1	3	1	3	TORN	**MAL2 Score**
	0.2979	0.0683	0.1025	0.0254	0.3177	0.1844	0.5083	0.1005	0.547		**MAL2 Reads**
	0.0104	0.0183	0.0084	0.0208	0.0137	0.0158	0.0147	0.0260	0.0062		**GZMB Reads**
I	**IDC**	**IDC**	**IDC**	**IDC**	**IDC**	**IDC**	**IDC**	**IDC**	**IDC**	**IDC**	
	T2N1M0	T2N0M0	T2N1M0	T2N0M0	T2N0M0	T2N0M0	T2N0M0	T2N1M0	T1N0M0	T2N0M0	
	3	1	2	1	1	Artifact	1	1	3	3	**MAL2 Score**
	0.4463	0.0617	0.3272	0.2688	0.1063		0.1613	0.1638	0.3979	0.3531	**MAL2 Reads**
	0.0060	0.0179	0.0113	0.0093	0.0260		0.0240	0.0425	0.0040	0.0067	**GZMB Reads**
J	**IDC**	**IDC**	**IDC**	**IDC**	**IDC**	**IDC**	**IDC**	**IDC**	**IDC**	**IDC**	
	T2N1M0	T2N0M0	T2N0M0	T3N1M0	T3N0M0	T2N1M0	T2N0M0	T2N2M0	T4N0M0	T3N1M0	
	2	+/-	3	3	3	+/-	3	2	3	TORN	**MAL2 Score**
	0.2780	0.0461	0.4342	0.4626	0.5872	0.1815	0.4828	0.2975	0.3670		**MAL2 Reads**
	0.01555	0.03536	0.0101	0.0163	0.0077	0.0130	0.0089	0.0117	0.0215		**GZMB Reads**
K	**NORMAL**	**NORMAL**	**NORMAL**	**NORMAL**	**NORMAL**	**NORMAL**	**NORMAL**	**NORMAL**	**NORMAL**	**NORMAL**	
	TORN	S/F/M	Neg	Neg	TORN	Neg	S/F/M	Neg	Neg	TORN	**MAL2 Score**
			0.0065	0.0260		0.0222		0.0269	0.0262		**MAL2 Reads**

			0.0144	0.0358		0.0121		0.0094	0.0282		**GZMB Reads**

IDC: invasive ductal carcinoma

* S/F/M: Stroma/Fat/MSC

3R1503f

	1	2	3	4	5	6	7	8	9	10	11	12	13	14	15	
A	NORMAL	NORMAL	NORMAL	NORMAL	NORMAL	NORMAL	Fibroadenoma	Fibroadenoma	Fibroadenoma	Fibroadenoma	Fibroadenoma	Fibroadenoma	L.M.C.P	L.M.C.P	L.M.C.P	
	Neg	Neg	Neg	TORN	Neg	Neg	TORN	TORN	Neg	+/-	Neg	+/-	+/-	+/-	Neg	**MAL2 Score**
	0.0016	0.0018	0.0008		0.0004	0.0004			0.0034	0.0100	0.0103	0.0093	0.0064	0.0474	0.0037	**MAL2 Reads**
	0.0379	0.0231	0.0445		0.0758	0.0448			0.0282	0.0329	0.0341	0.0315	0.0202	0.0302	0.0091	**GZMB Reads**
B	L.M.C.P	IDC	IDC	IDC	IDC	IDC	IDC	IDC	IDC	IDC	IDC	IDC	IDC	IDC	IDC	
		TisN0M0	TisN0M0	TisN0M0	TisN0M0	TisN0M0	TisN0M0	TisN0M0	TisN0M0	TisN0M0	TisN0M0	TisN0M0	TisN0M0	TisN0M0	TisN0M0	
	+/-	Neg	1	1	1	TORN	TORN	2	1	1	1	1	2	1	TORN	**MAL2 Score**
	0.0313	0.0048	0.1482	0.0829	0.1238			0.1890	0.0669	0.0678	0.1097	0.0945	0.1964	0.0871		**MAL2 Reads**
	0.0169	0.0173	0.0381	0.0168	0.0072			0.0203	0.0308	0.0496	0.0576	0.0305	0.0238	0.0658		**GZMB Reads**
C	IDC	IDC	IDC	IDC	IDC	IDC	IDC	IDC	IDC	IDC	IDC	IDC	IDC	IDC	IDC	
	T3N1M0	T3N1M0	T2N0M0	T2N0M0	T3N0M0	T3N0M0	T2N0M0	T2N0M0	T4N2M0	T4N2M0	T2N0M0	T2N0M0	T2N0M0	T2N0M0	T3N0M0	
	1	1	1	2	2	TORN	1	1	TORN	1	1	1	1	1	1	**MAL2 Score**
	0.1340	0.1586	0.0448	0.1332	0.0880		0.0725	0.0885		0.0814	0.0713	0.1246	0.0730	0.0769	0.0471	**MAL2 Reads**
	0.0828	0.0433	0.0110	0.0067	0.0177		0.0254	0.0388		0.0915	0.0180	0.0194	0.0497	0.0339	0.0245	**GZMB Reads**
D	IDC	IDC	IDC	IDC	IDC	IDC	IDC	IDC	IDC	IDC	IDC	IDC	IDC	IDC	IDC	
	T3N0M0	T4N0M0	T4N0M0	T2N2M0	T2N2M0	T2N0M0	T2N0M0	T2N0M0	T2N0M0	T2N0M0	T2N0M0	T3N2M0	T3N2M0	T2N2M0	T2N2M0	
	1	2	2	2	3	3	2	3	3	3	3	1	1	2	1	**MAL2**

																Score
	0.0688	0.2304	0.1748	0.2146	0.4372	0.3449	0.2180	0.4445	0.3068	0.2340	0.2653	0.0450	0.0387	0.1103	0.0906	**MAL2 Reads**
	0.0328	0.0121	0.0185	0.0171	0.0060	0.0050	0.0144	0.0154	0.0251	0.0212	0.0166	0.0667	0.0682	0.0210	0.0213	**GZMB Reads**
E	IDC	IDC	IDC	IDC	IDC	IDC	IDC	IDC	IDC	IDC	IDC	IDC	IDC	IDC	IDC	
	T2N2M0	T2N2M0	T4N1M0	T4N1M0	T2N1M0	T2N1M0	T2N1M0	T2N1M0	T2N2M0	T2N2M0	T3N0M0	T3N0M0	T2N2M0	T2N2M0	T4N0M0	
	1	2	+/-	+/-	1	TORN	3	3	1	1	2	1	2	1	1	**MAL2 Score**
	0.1090	0.1950	0.0296	0.0106	0.1021		0.4184	0.4018	0.1057	0.0878	0.1958	0.0943	0.1684	0.0710	0.0768	**MAL2 Reads**
	0.0527	0.0233	0.0335	0.0174	0.0718		0.0140	0.0153	0.0336	0.0349	0.0389	0.0450	0.0131	0.0150	0.0281	**GZMB Reads**
F	IDC	IDC	IDC	IDC	IDC	IDC	IDC	IDC	IDC	IDC	IDC	IDC	IDC	IDC	IDC	
	T4N0M0	T2N0M0	T2N0M0	T2N1M0	T2N1M0	T2N2M0	T2N2M0	T2N1M0	T2N1M0	T4N2M0	T4N2M0	T2N0M0	T2N0M0	T2N0M0	T2N0M0	
	2	2	2	1	1	3	3	1	1	+/	1	1	+/-	Neg	1	**MAL2 Score**
	0.1049	0.2589	0.2990	0.1273	0.2410	0.3568	0.2355	0.1640	0.1865	0.0270	0.0466	0.1269	0.0046	0.0042	0.0550	**MAL2 Reads**
	0.0339	0.0171	0.0096	0.0306	0.0280	0.0039	0.00356 2	0.0173	0.0164	0.0788	0.0436	0.0455	0.0420	0.0495	0.0212	**GZMB Reads**
G	IDC	IDC	IDC	IDC	IDC	IDC	IDC	IDC	IDC	IDC	IDC	IDC	IDC	IDC	IDC	
	T2N0M0	T2N0M0	T3N1M0	T3N1M0	T3N0M0	T3N0M0	T1N0M0	T1N0M0	T2N0M0	T2N0M0	T4N0M0	T4N0M0	T1N0M0	T1N0M0	T2N0M0	
	+/-	1	2	2	2	2	2	+/-	+/-	+/-	Neg	2	1	1	1	**MAL2 Score**
	0.0922	0.1974	0.1949	0.1385	0.3642	0.3890	0.1990	0.0791	0.0815	0.0172	0.1762	0.1300	0.0533	0.0924	0.0657	**MAL2 Reads**
	0.0360	0.0162	0.0079	0.0045	0.0142	0.0101	0.0098	0.0194	0.0748	0.0236	0.0237	0.0200	0.0336	0.0283	0.0079	**GZMB Reads**
H	IDC	IDC	IDC	IDC	IDC	IDC	IDC	IDC	IDC	IDC	IDC	IDC	IDC	IDC	IDC	

	T2N0M0	T2N0M0	T2N0M0	T2N1M0	T2N1M0	T3N1M0	T3N1M0	T2N0M0	T2N0M0	T4N0M0	T4N0M0	T2N0M0	T2N0M0	T3N0M0	T3N0M0	
	1	1	1	2	+/-	1	1	2	2	1	1	2	1	2	2	**MAL2 Score**
	0.1582	0.1639	0.0704	0.4120	0.1353	0.1118	0.1606	0.2936	0.1744	0.1125	0.1753	0.3218	0.2335	0.4801	0.5945	**MAL2 Reads**
	0.0092	0.0081	0.0073	0.0039	0.0093	0.0042	0.0058	0.0125	0.0161	0.0193	0.0218	0.0191	0.0214	0.0147	0.0097	**GZMB Reads**
I	IDC	IDC	IDC	IDC	IDC	IDC	IDC	IDC	IDC	IDC	IDC	IDC	IDC	IDC	IDC	
	T2N0M0	T2N0M0	T3N0M0	T3N0M0	T2N2M0	T2N2M0	T2N1M0	T2N1M0	T3N1M0	T3N1M0	T2N0M0	T2N0M0	T2N2M0	T2N2M0	T1N0M0	
	2	2	1	1	2	2	2	2	1	1	3	3	1	1	+/-	**MAL2 Score**
	0.1866	0.2014	0.0450	0.0653	0.2983	0.2505	0.1258	0.2275	0.0891	0.0753	0.4030	0.5715	0.1001	0.0752	0.0033	**MAL2 Reads**
	0.0070	0.0052	0.0159	0.0225	0.0127	0.0150	0.0162	0.0125	0.0339	0.0497	0.0140	0.0061	0.0081	0.0077	0.0137	**GZMB Reads**
J	IDC	IDC	IDC	IDC	IDC	IDC	IDC	IDC	IDC	IDC	IDC	IDC	IDC	IDC	IDC	
	T1N0M0	T2N0M0	T2N0M0	T3N0M0	T3N0M0	T2N0M0	T2N0M0	T2N2M0	T2N2M0	T4N2M0	T4N2M0	T2N0M0	T2N0M0	T3N0M0	T3N0M0	
	TORN	1	1	2	2	2	1	3	3	2	1	2	1	1	1	**MAL2 Score**
		0.0582	0.0498	0.3539	0.3354	0.1965	0.1332	0.4307	0.4259	0.1247	0.1336	0.1692	0.0660	0.1472	0.0974	**MAL2 Reads**
		0.0125	0.0105	0.0058	0.0077	0.0185	0.0320	0.0162	0.0199	0.0295	0.0312	0.0288	0.0303	0.0197	0.0189	**GZMB Reads**

Supplemental Table 5.

Summary of clinical, genetic and treatment features of the Patient-derived Organoids for Figure 9.

Sample No.	Case No.	Age	Gender	Prior Treatments	Genetic Status	Pathology Status	Grade
Patient #1	UH1908-22	42	F	Chemo	TNBC	primary	grade 3 (9/9)
Patient #2	UHB1909-06	71	F	None	TNBC	primary	grade 3 (9/9)

Supplemental Methods

Generation of Plasmid Constructs

Generation of Inducible Constructs

MAL2 shRNA plasmid kits from Millipore were used to deplete endogenous MAL2 in human or mouse cell lines. MAL2 inducible knockdown plasmids were constructed by cloning *MAL2* shRNA expression cassette into 5'*Xho*I and 3'*Mlu*I sites of pTRIPZ (GE Healthcare) under the control of tetracycline-inducible promoter.

Sequence of shRNA against mouse *Mal2*:

KD (TRCN0000100650):

5'-CCGGGCTGAATTTGAGTAACAGATTCTCGAGAATCTGTTACTCAAATTCAGCT TTTTG-3'

Sequence of shRNA against human *MAL2*:

KD-1(TRCN0000153726):

5'-CCGGCATAAACGTAGCAGCCTCAATCTCGAGATTGAGGCTGCTACGTTTATG TTTTTTG-3'

KD-2 (TRCN0000152286):

5'-CCGGCTTTATGACGACAGCTTGTTACTCGAGTAACAAGCTGTCGTCATAAAGT TTTTTG-3'

Expression plasmids for co-IP experiments

Human and mouse MAL2 overexpression plasmid, tagged with Flag and *c-Myc* at the amino terminus of MAL2, were purchased from OriGene Technologies (#RC203862, #MR216581). Plasmids expressing RAB7(#131417) and HLA-A (#100154) were obtained from Addgene. Plasmids expressing HA-RAB7A and Flag-RAB7A were constructed by subcloning *RAB7* cDNA fused with HA-tag or Flag-tag downstream of the CMV promoter using NheI and XhoI restriction sites in pDNA3.1.

mCherry-MAL2

The construct expressing mCherry-*MAL2* was generated by substituting the coding sequence of *centrin-1* from the pLVX-FLAG-mCherry-C1-*centrin-1* (Addgene, #73333) by that of the *MAL2* excised from the *MAL2* overexpression plasmid (OriGene Technologies).

MAL2 deletions and mutations

MAL2 mutation plasmids were generated from site-specific mutagenesis of human *MAL2* overexpression plasmid (#RC203862) using Q5® Site-Directed Mutagenesis Kit (New England

Biolabs, USA) with the primers (see the table below) designed by NEBaseChanger™ tool. Plasmid Flag- *MAL2*-N132A, Flag- *MAL2*-N144A, Flag- *MAL2*-N147A and Flag- *MAL2*-N149A were generated by introducing one point mutations (N132->A132, N144->A144, N147->A147, N149->A149) to human *MAL2* protein sequence, respectively. The Flag- *MAL2* 3N->3A mutant plasmid was constructed by introducing one point mutation at each of N144, N147, and N149 (N144->A144, N147->A147, N149->A149). The Flag- *MAL2* 4N->4A mutant was generated by introducing N132A mutation into the 3N->3A mutant.

Name (F/R)	Oligo
Flag- *MAL2*-N132A _ Forward	5'-TCATGCAGGGATGTGGCT-3'
Flag- *MAL2*-N132A _ Reverse	5'-TTTGCATTGCgctACAACCATAACCGGG-3'
Flag- *MAL2* 3N->3A_ Forward	5'-GCTATAGCTCGTAGCAGCCTCAATTTTTG-3'
Flag- *MAL2* 3N->3A_Reverse	5'-ATACTGAGCATCACTCAGGAGTGGCTG-3'
Flag- *MAL2*-N144A_ Forward	5'-CTGAGTGATgctCAGTATAACATAAACGTAGCAGC-3'
Flag- *MAL2*-N144A_ Reverse	5'- AGTGGCTGCCCGGTTATG -3'
Flag- *MAL2*-N147A_ Forward	5'-TAACCAGTATgctATAAACGTAGCAGCCTCAATTTTTG -3'
Flag- *MAL2*-N147A_ Reverse	5'- TCACTCAGGAGTGGCTGC-3'
Flag- *MAL2*-N149A_ Forward	5'-GTATAACATAgctGTAGCAGCCTCAATTTTTG-3'
Flag- *MAL2*-N149A_ Reverse	5'- TGGTTATCACTCAGGAGTG-3'

Quantitative PCR Analyses

Total cellular RNA was extracted from cells using TRIzol reagent (Invitrogen). First-strand cDNA was synthesized from the total RNA with random primers and subjected to PCR amplification with EX Taq polymerase (Takara).

MAL2 (human) Forward	5'-ACGTAGCAGCCTCAATTTTTGC-3'
MAL2 (human) Reverse	5'-CATCTTCGTAAAGCCAGACCC-3'
Mal2 (mouse) Forward	5'-GCTTTCGTCTGTCTGGAGATTG-3'
Mal2 (mouse) Reverse	5'-ACACAAACATGACCCATCCTTG-3'
H-2Kb (mouse) Forward	5'-CAGGTGGAGCCCGAGTATTG-3'
H-2Kb (mouse) Reverse	5'-CGTACATCCGTTGGAACGTG-3'
HLA-A (human) Forward	5'-GATTACATCGCCTTGAACGAGG-3'
HLA-A (human) Reverse	5'-AGAGACAGCGTGGTGAGTCAT-3'

Immunoblotting

Anti-MAL2 antibodies (p239 polyclonal and mAb 9D1) (1, 2) are kind gifts from Dr. M.A. Alonso (Centro de Biología Molecular Severo Ochoa, Consejo Superior de Investigaciones Científicas and Universidad Autónoma de Madrid, Madrid, Spain). Immunoblotting was performed as previously reported (3). Briefly, cultured cells were lysed on ice in pre-cold RIPA buffer (50 mM Tris, pH 7.4, 150 mM NaCl, 1% Nonidet P-40, 0.5% sodium deoxycholate, and 0.1% sodium dodecyl sulfate) supplemented with protease inhibitor Cocktail (Roche) and phosphatase inhibitor mixture (Thermo Scientific). After 20 minutes incubation, cell lysates were centrifuged and the pellets were removed, and the protein concentration was determined by BCA kit (Thermo Fisher Scientific). Membrane protein and cytoplasm protein were purified using Mem-PER™ Plus Membrane Protein Extraction Kit (Thermo Fisher Scientific). Tumor samples were also homogenized in the abovementioned RIPA buffer. Equal amounts of protein lysates were resolved by SDS–PAGE and transferred to PVDF membrane for western blot. The PVDF membrane was blocked with 5% non-fat milk and then incubated with primary antibody overnight at 4°C. After washing, the membrane was incubated with HRP-conjugated secondary antibody at a concentration of 1: 5,000-10,000 at room temperature for 1 hour. The results shown for each blot represent at least three independent experiments.

Co-immunoprecipitation

Co-immunoprecipitation (co-IP) was performed as described previously (4). Briefly, whole cell lysates were prepared by incubating cells in 0.5% NP-40 lysis buffer (0.5% NP-40, 20 mM Tris,

pH 7.4, 137 mM NaCl, 2 mM EDTA, 10% glycerol, and 1 mM PMSF with Roche cOmplete™ protease inhibitor cocktail) on ice for 30 minutes. After clearing by centrifugation at 16,000 x g at 4°C for 15 minutes, equal amounts of protein lysates were incubated with 2 µg of specific antibodies for 4 hours at 4°C. The immunoprecipitates (IP) were collected by incubation with protein A/G-agarose beads (Pierce) for 12 hours at 4°C followed by centrifugation and were then immunoblotted with the indicated antibodies. Antibodies used for immunoprecipitation were mouse anti-FLAG (MAB3118, Sigma-Aldrich), mouse anti-HA tag (ab18181, Abcam) and mouse anti-RAB7 (ab50533, Abcam).

Immunohistochemistry

Immunohistochemistry was carried out based on the protocol described in previous studies (5) with some modifications. Briefly, tissue samples were fixed in formalin overnight, washed with 70% ethanol and embedded in paraffin. Sections (3 µm) were prepared and processed for immunohistochemistry. For double-staining IHC, DoubleStain IHC Kit (ab210059, Abcam) was applied. Primary antibodies used were anti-mouse CD8 (#98941, Cell signaling Technology), anti-mouse cleaved caspase 3 (#9661, Cell signaling Technology) and anti-Ki-67 (ab15580, Abcam).

Human breast cancer tissue microarray (TMA):

The tissue microarray slides (BC081120e and BR1503f) were purchased from US Biomax at15883 Crabbs Branch Way, Derwood, MD 20855.

Two pathologists at Indiana University School of Medicine utilized light microscopy to evaluate the staining intensity of the tumor cells in each tissue core (6) (range from negative {Neg}, minimum {+/-}, [both {Neg} and {+/-} are considered as {0}], weak {+1}, moderate {+2}, or strong {+3}) on the *MAL2*stain. CD8 and *GZMB* were evaluated using immunoscoring.

Immunoscoring: Hand scores were performed by approximating immune cells in the entire area of each breast TMA core (including stroma and in-between tumor cell clusters) using a microscope. The IS (immune score) was expressed as negative, few, slight, moderate, or severe. Aperio positivities were then compared to the initial hand score, with immune cells making up less than 1%, 1-2.49%, 2.5-3.99%, 4-7.99%, and greater than 7.99%. Any discrepancies between the Aperio values and the hand score were re-evaluated to ensure accuracy and quality of tissue. Reference range for this immune score was compiled from over 2,000 previous breast TMA cores completed in immunology studies in previous years.

The Aperio whole slide digital imaging system was used for imaging. The Aperio Scan Scope CS system was used (360 Park Center Drive, Vista, CA 92081). The system imaged all slides at 20x. The scan time ranged from 1.5 minutes to a maximum time of 2.25 minutes.

The Positive Pixel Count Algorithm

The Positive Pixel Count algorithm was used to quantify the amount of a specific stain present in a scanned slide image. A range of color (range of hues and saturation) and three intensity ranges (weak, positive, and strong) were masked and evaluated.

The algorithm had a set of default input parameters when first selected—these inputs have been pre-configured for Brown color quantification in the three intensity ranges (220-175, 175-100, and 100-0).

The positive pixel count parameters were changed for each stain to allow for the analysis of one stain at a time. The following parameters are as follows:

MAL2 (excluding CD8) – Hue value = .946, Hue width = .05, Color saturation threshold = .131

MAL2 (excluding GZMB) – Hue value = .946, Hue width = .06, Color saturation threshold = .094

CD8 (excluding MAL2) – Hue value = .13, Hue width = .2, Color saturation threshold = .1

GZMB (excluding MAL2) – Used the same values as CD8.

The algorithm was applied to an image by using TMA Lab algorithm. This program allowed us to select an image Region of Analysis (set of spots in TMA Lab), specify the input parameters, run the algorithm, and view/save the algorithm results.

Quality Control:

With the data we compared each core (both path read and image analysis data) to arrive at a complete report. The QC process for the staining involved evaluating the {minimal, moderate, and strong} path read cores and matched against the image analysis data. Then we reexamined the {minimal and strong} path read cores against the image analysis data and negative cores on the path read against the imaging data for comparison and completion.

TNBC Transcriptomics Data Analysis

TCGA BRCA RNA-seq data were retrieved from Genomic Data Commons Data Portal. 115 TNBC samples were selected and the gene expression levels were normalized by FPKM. RNA-seq data of 398 METABRIC TNBC samples were downloaded from cbioprotal. Four microarray data sets of TNBC tissue samples (GSE18864, GSE32646, GSE58812, and GSE95700), totaling 363 samples, were retrieved from GEO database. Hazard ratio of the genes in TCGA BRCA data was

computed by using univariant cox regression model between patient overall survival and the log (FPKM+1) of each gene expression by using the "survival" R package. We further split the patients into *MAL2* high and low expression groups by median separation. Survival curves of the *MAL2* high and low patients were tested by log-rank test.

We utilized our recently developed deconvolution method, ICTD, to access cell proportions of T cell and other immune and stromal cell types. Specifically, ICTD identifies data set specific cell type uniquely expressed gene markers to optimize the estimation of cell proportion (7). In the collected TNBC tissue transcriptomics data, we identified high co-expression correlation among *CD2*, *CD3D*, *CD3E*, *CD3G*, and *CD8A* genes. The first eigen vector of the expression profile of these genes was utilized to estimate the relative proportion of total T cells in each sample. We further identified the T cell cytotoxicity marker genes *GZMA*, *GZMB*, *PRF1*, and *NKG7* were highly co-expressed in the samples with high predicted level of total T cells. The first eigen vector of the expression profile of these genes was utilized to estimate the whole tissue cytotoxicity level in the samples with high T cell level. Relative cytotoxicity level was computed by $Relative\ cytotoxicity\ level = \frac{Whole\ tissue\ cytotoxicity\ level}{Total\ T\ cell\ proportion}$. Genes in the downstream of T cell receptor signaling pathway were collected from Gene Ontology and Canonical Pathways from MSigDB. Complete list of the selected TCR downstream genes was given in Supplemental Table 1. Pearson correlation coefficients of *MAL2*, TCR downstream genes, and other genes with the relative proportion of T cell and other cell types, and the relative cytotoxicity level were computed. Genes top co-expressed with *MAL2* were computed. Pathway enrichment analysis of the top *MAL2* co-expressed genes was conducted by using Ingenuity Pathway Analysis.

Analysis of TNBC scRNA-seq Database

Single cell RNA sequencing of primary breast cancer (GE75688) was downloaded from GEO database. Single cells collected from TNBC microenvironment were selected and analyzed. Gene expression levels were normalized by TPM. Cell clustering was made and visualized by Seurat v3. Cell type label from the original paper was utilized and further confirmed by cell type specific markers genes. Expression levels of selected genes were visualized by the tSNE plot function encoded in Seurat 3.

Macropinosome visualization and quantification

For *in vitro* assay, cells were seeded on the 8-well Millicell® EZ glass slide (3,000 cells per well) and incubated overnight. Cells were the serum starved for 18 hours. Macropinosomes were

marked using a high-molecular-mass TMR-dextran (Invitrogen)-uptake assay wherein TMR-dextran was added to serum-free medium at a final concentration of 1 mg/mL for 30 minutes at 37 °C. Cells treated with EIPA (5-[N-ethyl-N-isopropyl] amiloride), a Na+/H+ exchanger (NHE) inhibitor that blocks macropinocytosis, served as negative controls (8). At the end of the incubation period, cells were rinsed five times in cold PBS and immediately fixed in 3.7% formaldehyde. Cells were DAPI-treated to stain nuclei and coverslips mounted onto slides using ProLong™ Gold Antifade Mountant (Invitrogen, Cat# P36930). Images were captured using a confocal fluorescent microscope (Leica) and analyzed using the 'Analyze Particles' feature in ImageJ (National Institutes of Health). The total particle area per cell was determined from at least three fields that were randomly selected from different regions across the entirety of each sample. For *in vivo* assay, EO771 cells were injected orthotopically into 5-week-old female C57/BL6 mice (Jackson Lab) at both flanks with 1 x 10^6 cells in a total volume of 50 µL. When tumors reached an average volume of 500 mm^3, 1 mg of fixable FITC-dextran (Invitrogen) diluted in PBS to a volume of 100 µL was injected intratumorally. At 2 hours post-injection, tumors were removed and rapidly frozen in tissue-freezing medium. Quantitative data are presented as mean ± SD of represented images from 5 parallel tumors.

Flow Cytometry

3 x10^6 cells per sample were stained with SYTOX™ Blue Dead Cell Stain (Thermofisher Scientific, S34857) according the manufacturer's instructions. Cells were then incubated in blocking solution containing 5% normal mouse serum and 5% normal rat serum in PBS and then stained with a standard panel of immunophenotyping antibodies (See in "Materials") for 30 minutes at room temperature. After staining, cells were washed and data was acquired with a BD Fortessa flow cytometer using BD FACSDiva software (BD Bioscience). Compensation was performed on the BD Fortessa flow cytometer at the beginning of each experiment. Data were analyzed using Flowjo v10. Cell sorting was performed on a BD Aria II.

Materials

REAGENT or RESOURCE	SOURCE	IDENTIFIER
Antibodies		
anti-MAL2 antibody, p239 polyclonal	(1)	

anti-MAL2 antibody, mAb 9D1	(2)	
anti-alpha Actinin 4 antibody [EPR2533(2)], rabbit monoclonal	Abcam	Cat# ab108198; RRID:AB_10858236
anti-HLA Class 1 ABC antibody [EMR8-5], mouse monoclonal	Abcam	Cat# ab70328; RRID:AB_1269092
anti-Na,K-ATPase antibody, rabbit	Cell Signaling Technology	Cat# 3010; RRID: AB_2060983
anti-GAPDH antibody [EPR16891], rabbit	Abcam	Cat# ab181602; RRID:AB_2630358
anti-DYKDDDDK Tag (D6W5B) antibody, rabbit monoclonal	Cell signaling Technology	Cat# 14793; RRID:AB_2572291
anti-HA Tag (C29F4) antibody, rabbit monoclonal	Cell signaling Technology	Cat# 3724; RRID:AB_1549585
anti-Rab7 (D95F2) antibody, rabbit monoclonal	Cell signaling Technology	Cat# 9367; RRID:AB_1904103
anti-HLA-A2 antibody, rabbit polyclonal	Abcam	Cat# ab168405
mouse Anti-DYKDDDDK (FLAG® epitope tag) (clone 2EL-1B11) antibody, mouse monoclonal	Sigma-Aldrich	Cat# MAB3118; RRID:AB_11213007
anti-HA tag antibody [HA.C5] , mouse monoclonal	Abcam	Cat# ab18181; RRID:AB_444303
anti-RAB7 antibody [Rab7-117], mouse monoclonal	Abcam	Cat# ab50533; RRID:AB_882241
anti-EGFR (D38B1) antibody, rabbit monoclonal	Cell Signaling Technology	Cat# 4267; RRID:AB_2246311
anti-EEA-1 (C45B10) antibody, rabbit monoclonal	Cell Signaling Technology	Cat# 3288; RRID:AB_2096811
anti-human LAMP-1 (D2D11) antibody, rabbit monoclonal	Cell Signaling Technology	Cat# 9091; RRID:AB_2687579
anti-mouse CD8a (D4W2Z) antibody, rabbit monoclonal	Cell Signaling Technology	Cat# 98941; RRID:AB_2756376
anti-cleaved caspase 3 (Asp175) antibody, rabbit polyclonal	Cell signaling Technology	Cat# 9661; RRID:AB_2341188
anti-Ki-67 antibody, rabbit polyclonal	Abcam	Cat# ab15580; RRID:AB_443209
InVivoMAb anti-mouse MHC Class I (H-2)	BioXcell	Cat# BE0077

		RRID: AB_1125537
InVivoMAb rat IgG2a isotype control	BioXcell	Cat# BE0089 RRID: AB_1107769
anti-EpCAM (E8Q1Z) Rabbit mAb (Mouse Preferred)	Cell signaling Technology	Cat# # 42515 RRID: BDSC_4251
APC anti-mouse H-2Kb bound to SIINFEKL antibody (25-D1.16)	Biolegend	Cat# 141605 RRID: AB_11219402
APC/Cy7 anti-human CD8a antibody (HIT8a)	Biolegend	Cat# 300926; RRID:AB_10613636
APC/Cy7 anti-mouse CD8a antibody (53-6.7)	Biolegend	Cat# 100714; RRID:AB_312753
FITC anti-mouse CD4 antibody (GK1.5)	Biolegend	Cat# 100405; RRID: AB_312690
APC anti-human IFN-γ antibody (4S.B3)	Biolegend	Cat# 502512; RRID:AB_315237
APC anti-mouse IFN-γ antibody (XMG1.2)	Biolegend	Cat# 505810; RRID:AB_315404
PE anti-human TNF-α antibody (MAb11)	Biolegend	Cat# 502909; RRID:AB_315261
PE anti-mouse TNF-α antibody (MP6-XT22)	Biolegend	Cat# 506306; RRID:AB_315427
PerCP/Cyanine5.5 anti-human/mouse Granzyme B Recombinant antibody (QA16A02)	Biolegend	Cat# 372212; RRID:AB_2728379
PE anti-mouse/human CD11b antibody (M1/70)	Biolegend	Cat# 101207; RRID: AB_312790
PE/Cyanine5 anti-mouse CD11c antibody (N418)	Biolegend	Cat# 117316; RRID: AB_493566
APC anti-mouse CD19 antibody (1D3/CD19)	Biolegend	Cat# 152409; RRID: AB_2629838
Brilliant Violet 605™ anti-mouse CD45 antibody (30-F11)	Biolegend	Cat# 103139; RRID: AB_2562341

PE/Cyanine7 anti-mouse F4/80 antibody (BM8)	Biolegend	Cat# 123113; RRID: AB_ 893490
Brilliant Violet 650™ anti-mouse I-A/I-E antibody (M5/114.15.2)	Biolegend	Cat# 107641; RRID: AB_2565975
PerCP/Cyanine5.5 anti-mouse Ly-6C antibody (HK1.4)	Biolegend	Cat# 128011; RRID: AB_1659242
Alexa Fluor® 700 anti-mouse Ly-6G antibody (1A8)	Biolegend	Cat# 127621; RRID: AB_10640452
siRNAs		
human *LRP11*	Sigma-Aldrich	Cat# EHU023481
human *PGK1*	Sigma-Aldrich	Cat# EHU105941
human *PCMT1*	Sigma-Aldrich	Cat# EHU041991
human *FAM173B*	Sigma-Aldrich	Cat# EHU048541
human *MAL2*	Sigma-Aldrich	Cat# EHU048681
Chemicals, Peptides, and Recombinant Proteins		
Proteinase K	Thermo Fisher Scientific	Cat# 25530049
Lipofectamine 3000 reagent	Thermo Fisher Scientific	Cat# L3000-008
Pierce Protease Inhibitor Tablets	Thermo Fisher Scientific	Cat# A32963
Protease inhibitor Cocktail	Abcam	Cat# ab65621
Premix WST-1 Cell Proliferation Assay System	Takara	Cat# MK400
DynabeadsTM Protein G	Thermo Fisher Scientific	Cat# 10003D
DynabeadsTM Protein A	Thermo Fisher Scientific	Cat# 10001D
Critical Commercial Assays		
RNeasy mini-isolation kit	QIAGEN	Cat# 74106
QIAquick Gel Extract kit	QIAGEN	Cat# 28706

QIAquick PCR purification kit	QIAGEN	Cat# 28106
QIAprep Spin Miniprep Kit	QIAGEN	Cat# 27106
QIAGEN Plasmid Plus Maxi Kit	QIAGEN	Cat# 12965
ELISA MAX™ Deluxe Set Human TNF-α	Biolegend	Cat# 430204
ELISA MAX™ Deluxe Set Mouse TNF-α	Biolegend	Cat# 430904
ELISA MAX™ Deluxe Set Human IFN-γ	Biolegend	Cat# 430104
ELISA MAX™ Deluxe Set Mouse IFN-γ	Biolegend	Cat# 430804
CytoTox 96® Non-Radioactive Cytotoxicity Assay	Promega	Cat# G1780
CD8 MicroBeads, human	Miltenyi Biotec	Cat# 130-045-201
CD8 (TIL) MicroBeads, mouse	Miltenyi Biotec	Cat# 130-116-478
Duolink® In Situ Red Starter Kit Mouse/Rabbit	Sigma	Cat# DUO92101-1KT
Trident Endosome Isolation Kit	GeneTex	Cat# GTX35192
Mem-PER™ Plus Membrane Protein Extraction Kit	Thermo Fisher Scientific	Cat# 89842
Fast SYBR™ Green Master Mix	Thermo Fisher Scientific	Cat# 4385610
Human Paraffin Embedded Tissue Array		
Breast cancer array with adjacent normal breast tissue, including pathology grade, TNM, clinical stage and IHC markers (ER, PR and Her-2), 110 cases/110 cores	Biomax.us	Cat# BC081120e
Breast cancer tissue array, including TNM and pathology grade, with IHC results of Her-2\ER\PR\Ki67, 75 cases/ 150 cores	Biomax.us	Cat# BR1503f
Cell Lines and Antigen Specific T Cell		
MDA-MB-468	ATCC	Cat# HTB-132; RRID: CVCL_0419
HCC1954	ATCC	Cat# CRL-2338; RRID: CVCL_1259
HEK293T	ATCC	Cat# CRL-3216; RRID: CVCL_0063

EO771	CH3 BioSystems	Cat# 940001; RRID: CVCL_GR23
4T1	ATCC	Cat# 2539; RRID: CVCL_0125
anti-NY-ESO-1 T cells	Cellero	Cat # 1093-4493OC19
anti-MAGE A10 T cells	Cellero	Cat # 1125-4530DE19
Software and Algorithms		
R	N/A	https://www.r-project.org/
ImageJ	NIH	https://imagej.nih.gov/ij/
GraphPad Prism 7.0	GraphPad	https://www.graphpad.com/
Gene Set Enrichment Analysis (GSEA)	(9)	http://software.broadinstitute.org/gsea/

References in Supplemental Methods

1. Yu MJ, Pisitkun T, Wang G, Aranda JF, Gonzales PA, Tchapyjnikov D, et al. Large-scale quantitative LC-MS/MS analysis of detergent-resistant membrane proteins from rat renal collecting duct. *Am J Physiol Cell Physiol.* 2008;295(3):C661-78.
2. de Marco MC, Martin-Belmonte F, Kremer L, Albar JP, Correas I, Vaerman JP, et al. MAL2, a novel raft protein of the MAL family, is an essential component of the machinery for transcytosis in hepatoma HepG2 cells. *J Cell Biol.* 2002;159(1):37-44.
3. Liu Y, Zhang X, Han C, Wan G, Huang X, Ivan C, et al. TP53 loss creates therapeutic vulnerability in colorectal cancer. *Nature.* 2015;520(7549):697-701.
4. Fang Y, Chen Y, Yu L, Zheng C, Qi Y, Li Z, et al. Inhibition of breast cancer metastases by a novel inhibitor of TGFbeta receptor 1. *Journal of the National Cancer Institute.* 2013;105(1):47-58.
5. Li Y, Liu Y, Xu H, Jiang G, Van der Jeught K, Fang Y, et al. Heterozygous deletion of chromosome 17p renders prostate cancer vulnerable to inhibition of RNA polymerase II. *Nat Commun.* 2018;9(1):4394.
6. Adams S, Loi S, Toppmeyer D, Cescon DW, De Laurentiis M, Nanda R, et al. Pembrolizumab monotherapy for previously untreated, PD-L1-positive, metastatic triple-negative breast cancer: cohort B of the phase II KEYNOTE-086 study. *Ann Oncol.* 2019;30(3):405-11.
7. Chang W, Wan C, Zhang Y, So K, Richardson B, Sun Y, et al. ICTD: Inference of cell types and deconvolution -- a next generation deconvolution method for accurate assess cell population and activities in tumor microenvironment. *bioRxiv.* 2018:426593.
8. Commisso C, Davidson SM, Soydaner-Azeloglu RG, Parker SJ, Kamphorst JJ, Hackett S, et al. Macropinocytosis of protein is an amino acid supply route in Ras-transformed cells. *Nature.* 2013;497(7451):633-7.
9. Subramanian A, Tamayo P, Mootha VK, Mukherjee S, Ebert BL, Gillette MA, et al. Gene set enrichment analysis: a knowledge-based approach for interpreting genome-wide expression profiles. *Proceedings of the National Academy of Sciences of the United States of America.* 2005;102(43):15545-50.

Uncropped immunoblots

Figure 5D

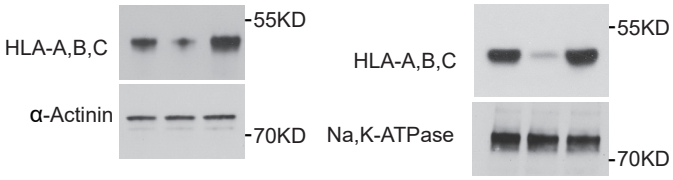

Figure 7A

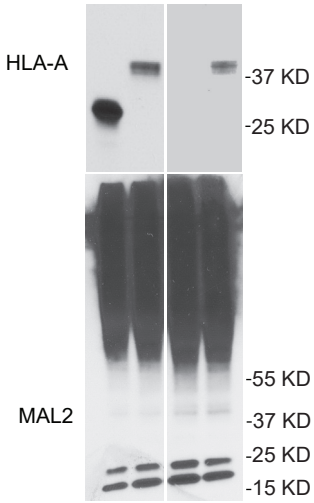

Figure 7B

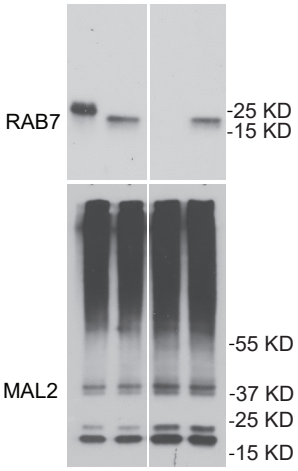

Figure 7C

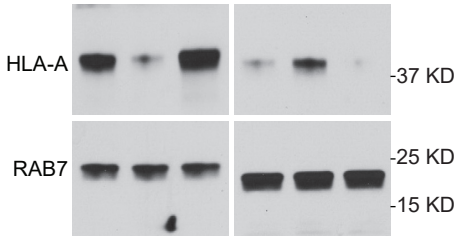

Figure 7E

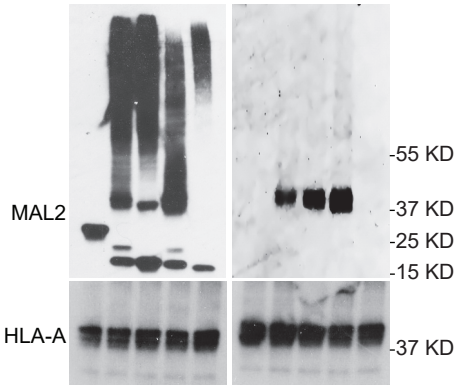

Supplemental Figure 1A

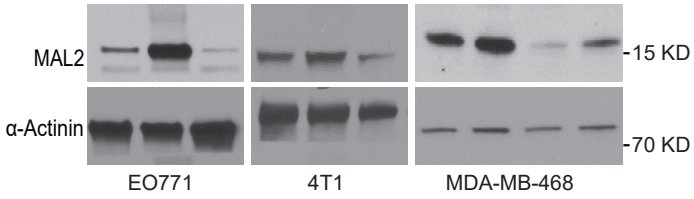

Supplemental Figure 3D

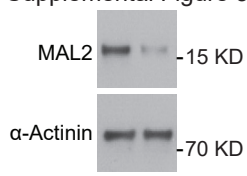

Supplemental Figure 5A

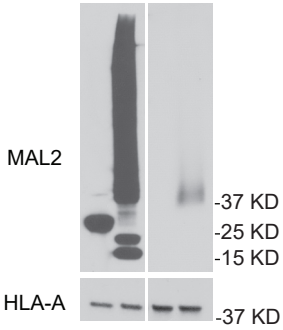

Supplemental Figure 5B

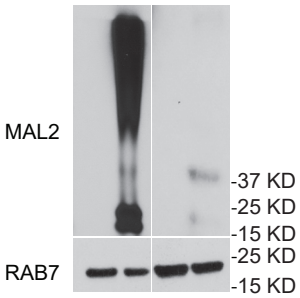

Supplemental Figure 5D

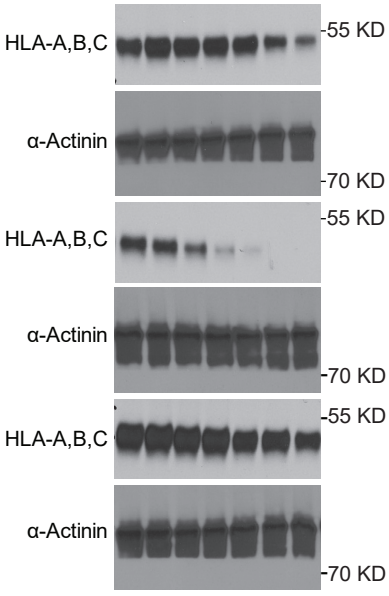

Supplemental Figure 4B

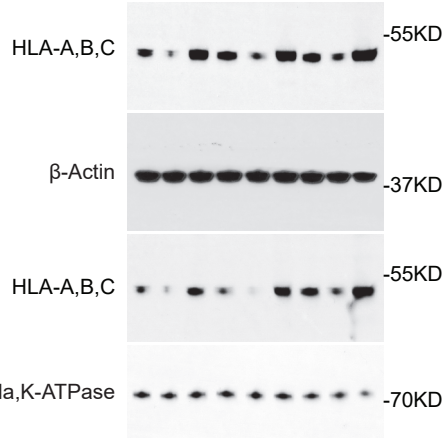

Supplemental Figure 5C